




RL10 GIMBAL FRICTION TEST

FINAL REPORT

CONTRACT NAS3-23313

Prepared for
National Aeronautics and Space Administration
Lewis Research Center
21000 Brookpark Road
Cleveland, Ohio 44135

Approved by: 
for J. R. Brown
Program Manager

Prepared by
United Technologies Corporation
Pratt & Whitney
Government Products Division
P.O. Box 109600, West Palm Beach, Florida 33410-9600



FOREWORD

This report presents the assessment and work done to investigate the gimbal friction of the RL10 rocket engine. The fixture design and setup, along with testing, evaluation, and recommendations, are presented. The testing was conducted by Pratt & Whitney, Government Products Division (P&W/GPD) of the United Technologies Corporation (UTC) for the National Aeronautics and Space Administration Lewis Research Center (NASA/LeRC) under contract NAS3-23313 Change Order 8. The testing effort was conducted under the direction of LeRC Space Flight Systems Directorate with Mr. James A. Burkhart as Contracting Officer Representative. The effort at P&W/GPD was carried out by Mr. Michael C. Calandra and Mr. Steven D. Gyrsting as principal investigators. The principal investigator at NASA/LeRC was Mr. James W. Askew.

ABSTRACT

Due to changes in the Centaur upper stage vehicle requirements, low gain autopilot performance showed that flight control depended on the friction characteristics of the Pratt & Whitney (P&W) RL10 engine gimbal system. The NASA Lewis Research Center (LeRC) began an investigation into the friction characteristics of the RL10 gimbal with P&W. Pratt & Whitney designed and built a test rig to measure forces required to rotate the gimbal under a simulated thrust load of 15,000 lb-force and in the expected altitude/thermal environment. Tests were performed at ambient temperature and pressure of 75°F, 14.7 psi, ambient temperature and vacuum of 75°F, 5.9×10^{-6} psi, and flight temperature and vacuum of -290°F, 5.9×10^{-6} psi. This report describes the rig, method of test, and problems associated with the testing of an RL10 gimbal.

CONTENTS

<i>Section</i>	<i>Page</i>
1.0 INTRODUCTION	1
2.0 DESIGN AND FUNCTION OF THE TEST FIXTURE	2
3.0 FIXTURE SETUP AND INITIAL CHECKOUT	11
4.0 DEVELOPMENT TESTING	14
5.0 PRODUCTION CYCLING	17
6.0 CONCLUSIONS	18
7.0 RECOMMENDATIONS	19
APPENDIX A — Strain Gage Calibration	A-1
APPENDIX B — TC Channel (°F).....	B-1
APPENDIX C — Reference Memos	C-1
APPENDIX D — Gimbal Test Fixture Drawings	D-1
APPENDIX E — Centaur Engine Gimbal Friction Characteristics Under Simulated Thrust Load	E-1

SECTION 1.0 INTRODUCTION

As part of the RL10 Shuttle/Centaur engine program, Contract NAS3-23313 Mod 8 was added to design and build a test fixture for measuring gimbal friction. The test fixture was designed to measure the gimbal friction forces under a simulated engine thrust load and in a temperature/vacuum environment which simulated flight conditions. This investigation was due to anticipated flight control problems with a low gain autopilot when using the gimbal friction value of 220 ft-lb presented in the engine model specification. It was believed that the friction was significantly lower and therefore needed to be measured and input to the autopilot system. The fixture was designed and built by Pratt & Whitney to be used in the NASA LeRC vacuum facility, Super Bell Jar, located in the Electronic Propulsion Laboratory (EPL).

The test fixture was built and shipped to NASA LeRC in August 1985. Stand installation and setup began in September 1985 and final testing ended in early November 1985. Three development and three production gimbals were tested. From the three production gimbals, two were selected to be placed on flight engines P642045 and P642046 and the third was placed in storage as a spare.

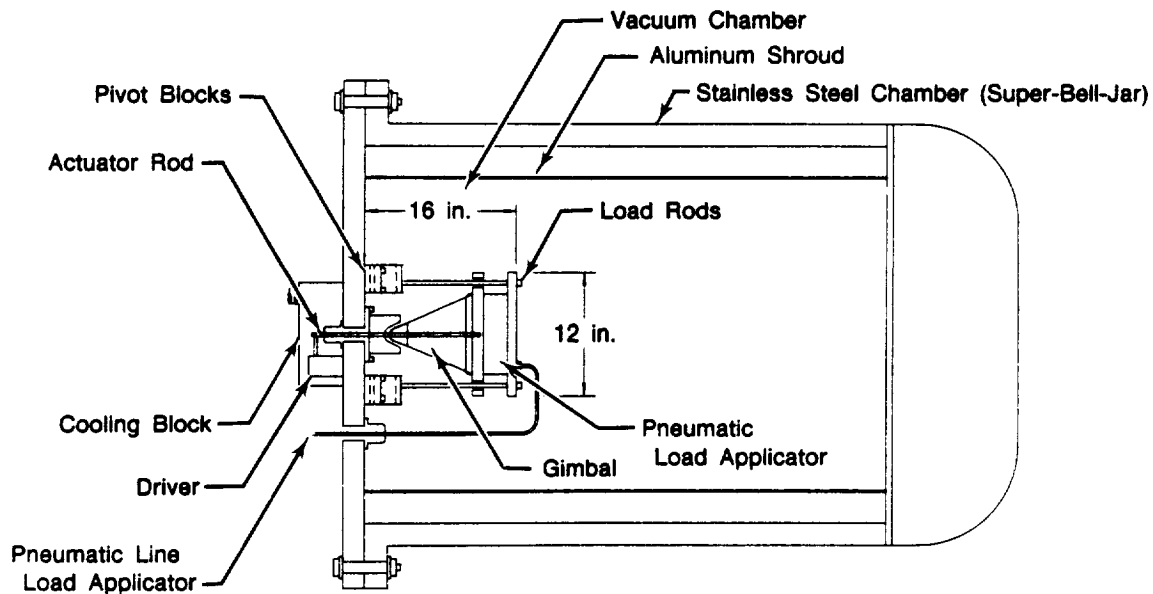
This report summarizes the design and testing that took place. All gimbal analysis was done by NASA and can be found in NASA Technical Memorandum 87335, June 1986. This report describes the accomplishments made from April 1985 through November 1985. Steve D. Gyrsting and Michael C. Calandra are co-authors of this report.

SECTION 2.0 DESIGN AND FUNCTION OF THE TEST FIXTURE

Design requirements for the test fixture were to simulate the environment and thrust load at which the gimbal functions, and to measure the gimbal friction under these conditions. The conditions for which the test fixture was designed are:

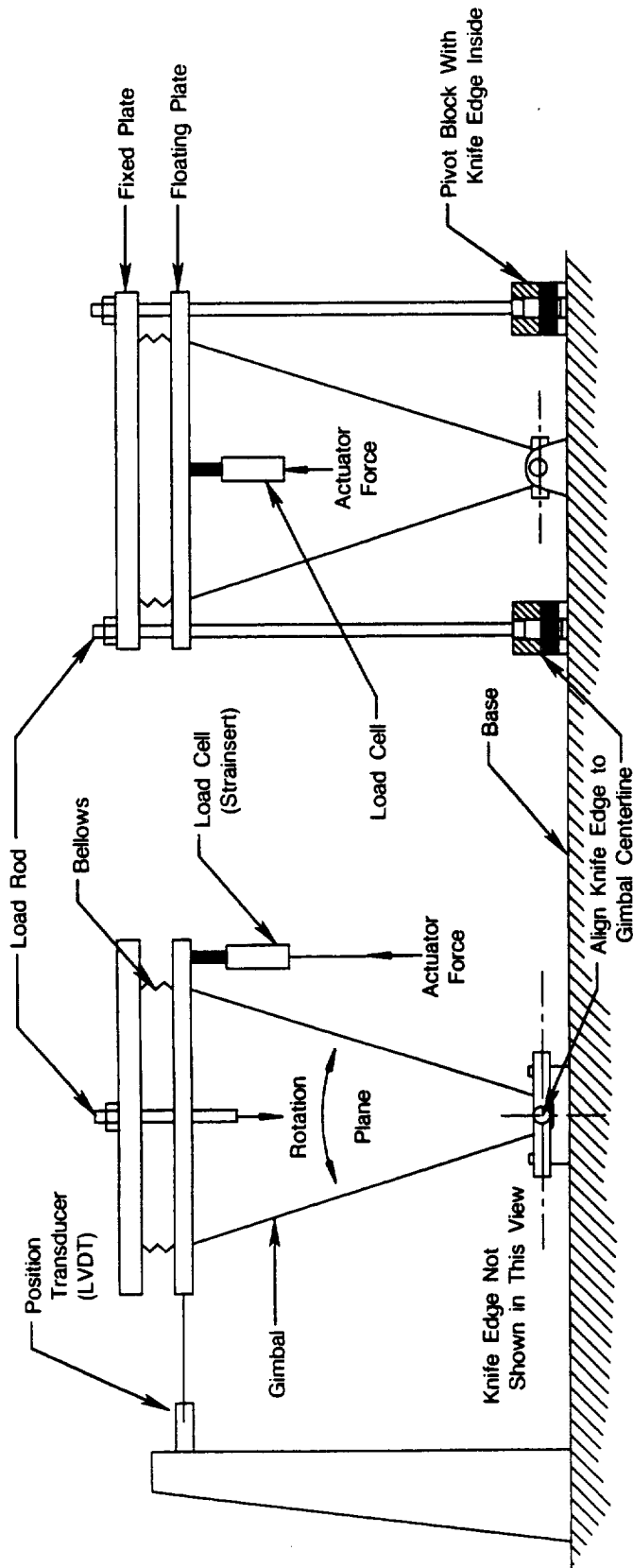
- Vacuum up to 10^{-8} Torr
- Simulated thrust load of 15,000 lb-force
- Simulate mounting to LOX tank with a 175°R temperature
- Measure gimbal friction with at least 10 percent accuracy
- Minimize test fixture friction so as not to interfere with gimbal friction
- Designed to be placed in Super Bell Jar at NASA-LeRC.

The test rig was designed at P&W with most of the manufactured hardware produced by Skillmetric Machine Co. of Delray Beach, FL. The rig baseplate is 40-inch diameter by 1-inch thick steel with a 9-inch diameter hole in the center. An aluminum cooling block on which the gimbal to be tested is mounted is inserted into the center hole. This block contains passages through which LN_2 can be flowed to maintain the gimbal mount temperature of approximately 175°R to simulate engine mounting to the vehicle oxygen tank. This entire plate forms the end closure of the cylindrical Super Bell Jar chamber; see Figures 1 and 2.



FD 320167

Figure 1. Gimbal Friction Measurement Test Setup



FDA 320168

Figure 2. Gimbal Friction Test Rig Configuration

Attached to the baseplate are two pivot blocks that contain 0.040R knife edges. The minimum friction knife edges are used as the rig pivot points. The knife edges are used to minimize the fixture friction and are placed on the gimbal centerline to prevent changes in loading during gimbal rotation. The knife edges allow the gimbal to rotate a maximum of ± 2.25 degrees, while under the simulated 15,000 lb thrust load. Only one axis of rotation was designed into the rig because the gimbal can be rotated 90 degrees to test the other axis.

The load rods are attached to the pivot blocks. Each load rod contained a thermocouple (TC) and a calibrated strain gage to measure load rod temperature change and load placed on the gimbal. The TC is used to provide correction to the strainage loads as a function of the temperature change. A pneumatic actuator was placed between two plates at the gimbal base to provide the force that simulates the thrust of the rocket engine, see Figure 1. This load traps the gimbal between the top floating plate and the aluminum cooling block. This pneumatic load application system was designed to permit remote load application needed to simulate engine thrust load after a long coast period with no load.

A Strainsert load cell used to measure the load applied for rotation is mounted on the actuator rod that is attached to the top plate of the dual plate loading system. This actuator rod is passed through the steel plate by using a Teflon bellows as a seal. Passing the actuator rod to the outside of the vacuum chamber allows a standard-type actuator to be used. A hydraulic Moog valve was chosen to actuate the gimbal for the testing. The actuator permitted rotation of the gimbal around positions from null to ± 2 degrees. The gimbal can be oscillated about these positions at an amplitude of ± 0.25 degree and at frequencies ranging from 0.04 to 10 Hz and waveforms of triangle, sinusoidal or square. Greater amplitudes are possible at positions closer to null, but total gimbal rotation cannot exceed 2.25 degrees.

The hydraulic actuator contains its own position indicator, a linear variable displacement transducer (LVDT). However, for accuracy purposes a more sensitive LVDT was placed in the rotation plane of the gimbal and attached to the loading plate. This LVDT allows accurate position indication and closed-loop control of the gimbal testing. The accuracy of the LVDT was 0.001 inch when the gimbal movement was ± 0.027 inch. (This corresponds to an amplitude of oscillation of ± 0.25 degree).

Simulation of the gimbal environment and proximity to the vehicle liquid oxygen (LOX) tank was considered important. Five TCs were installed on the test fixture and gimbal for control of this environment and monitoring of gimbal temperature. Three TCs were added later to provide additional information of the temperature profile of the load rods. The concern was that in a long temperature soak, the temperature of the load rods changed enough to affect the strainage calibration. These temperature readings were then used to correct the reading. See Table 1 and Figures 3 and 4 for parameters and locations.

Table 1. TC Channel Assignments

TC No.	Status	Location
0	Original	Gimbal Pivot Base, B-side
1	Original	Load Rod Base, A-side
2	Original	Load Rod Base, B-side
3	Original	Mid Gimbal
4	Original	Gimbal Pivot Base, A-side
5	Added Later	Load Rod A
6	Added Later	Load Rod B
7	Added Later	Base Plate

0354C

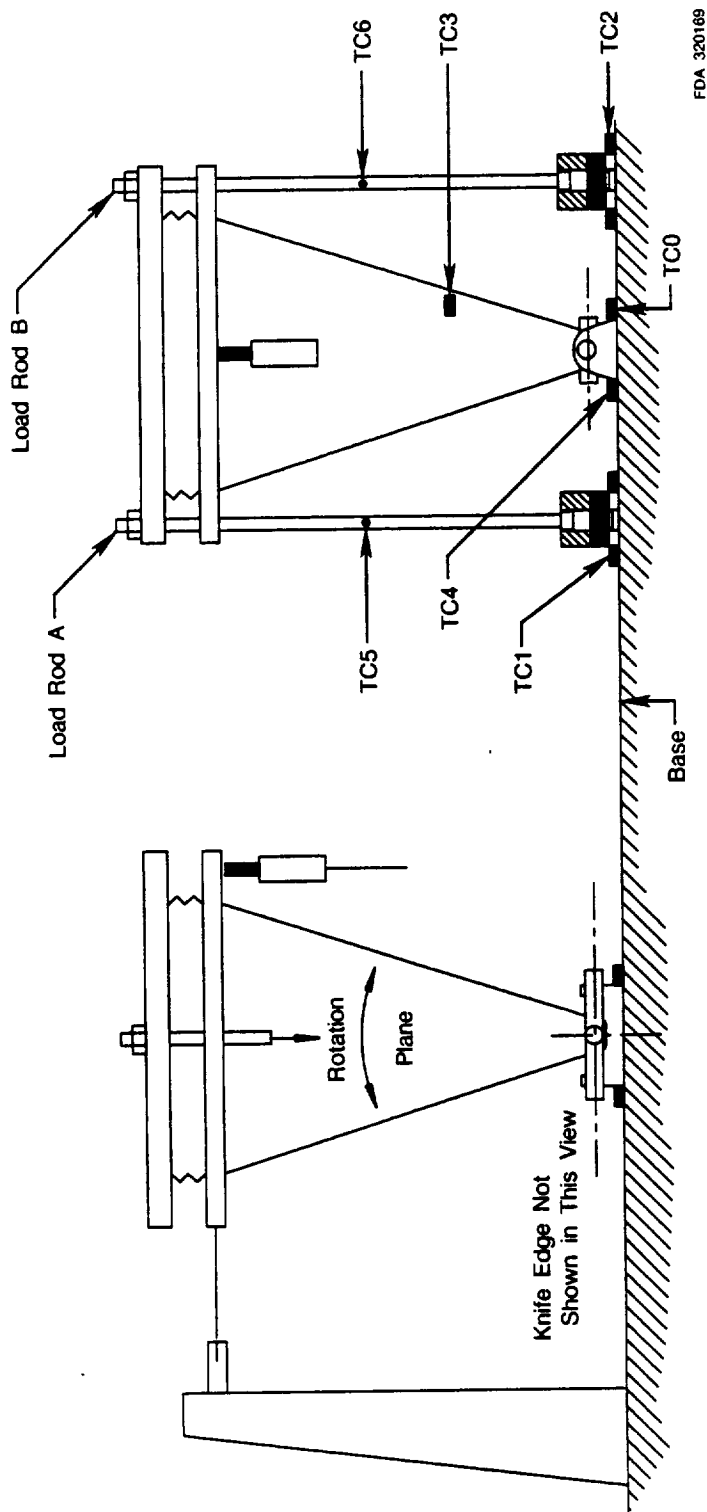
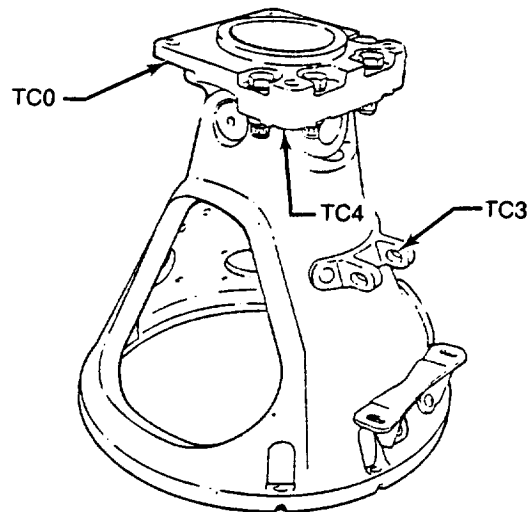


Figure 3. Thermocouple Locations



FD 320170

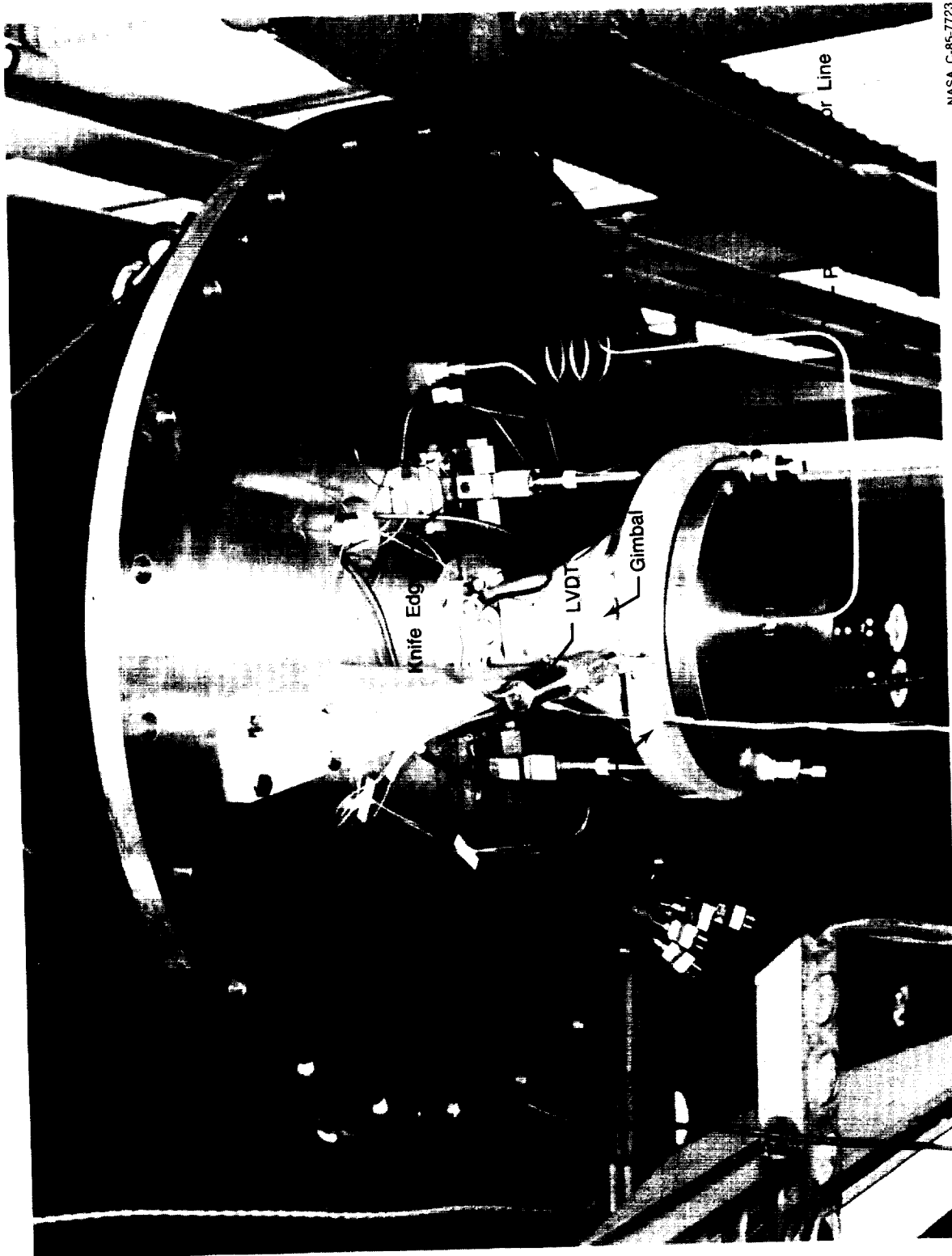
Figure 4. Engine Mount Gimbal Assembly

Figures 5 through 8 show the test fixture during testing at NASA LeRC.

All instrumentation was reviewed by P&W instrumentation engineers for accuracy and to ascertain that it would meet the design requirements. The results are presented in Appendix C, References 1, 2, and 3.

A dummy gimbal, shown installed in the test fixture in Figure 8, incorporating a set of knife edges, was used to test rig operation and for calibration of the fixture. The knife edges were the same material, design and area of the test fixture knife edges. The dummy gimbal allowed for the measurement of the knife edge friction and calibration of the friction levels in the fixture which could then be subtracted from the recorded friction loads of the real gimbal.

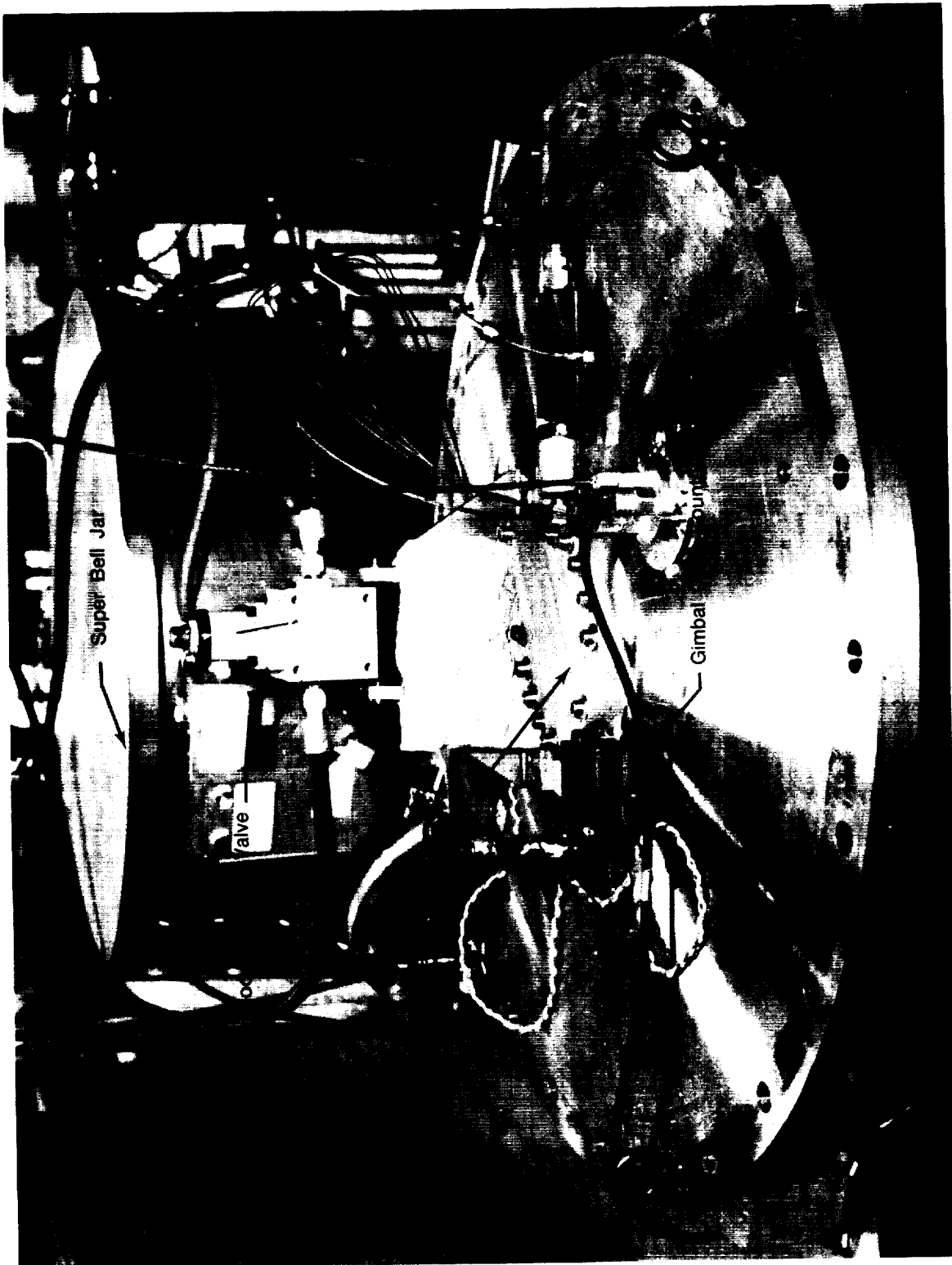
Prior to finalizing the design, an internal design review was conducted at P&W by the chief engineer's office. No major design problems were found. During that review, recommendations were made for an alternate fixture design and for additional friction investigations, however, it was decided not to pursue these at that time. The results of the design review are presented in Appendix C, Reference 4.



NASA C-85-7723

FD 320171

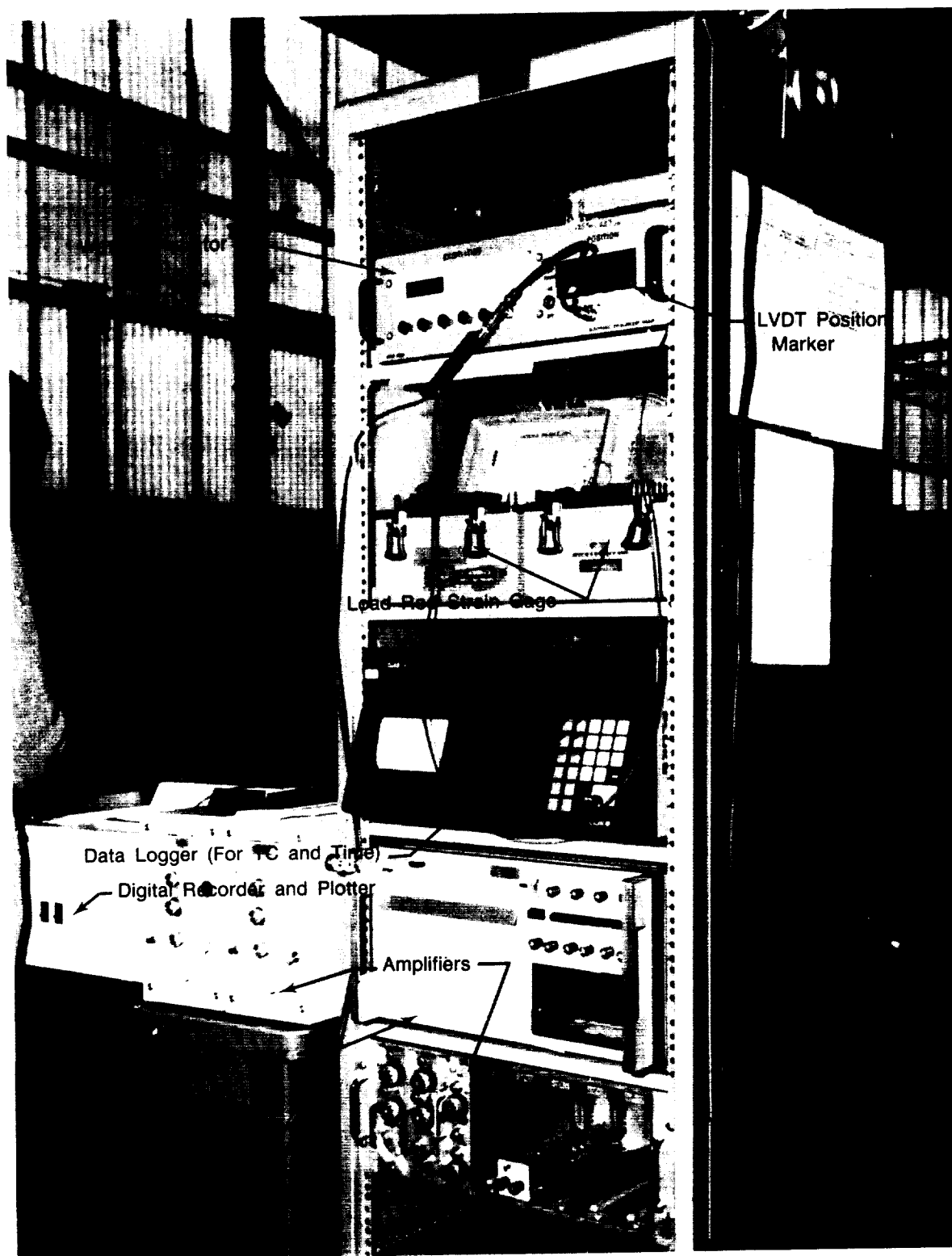
Figure 5. Vacuum Side of Test Fixture



NASA C-85-7721

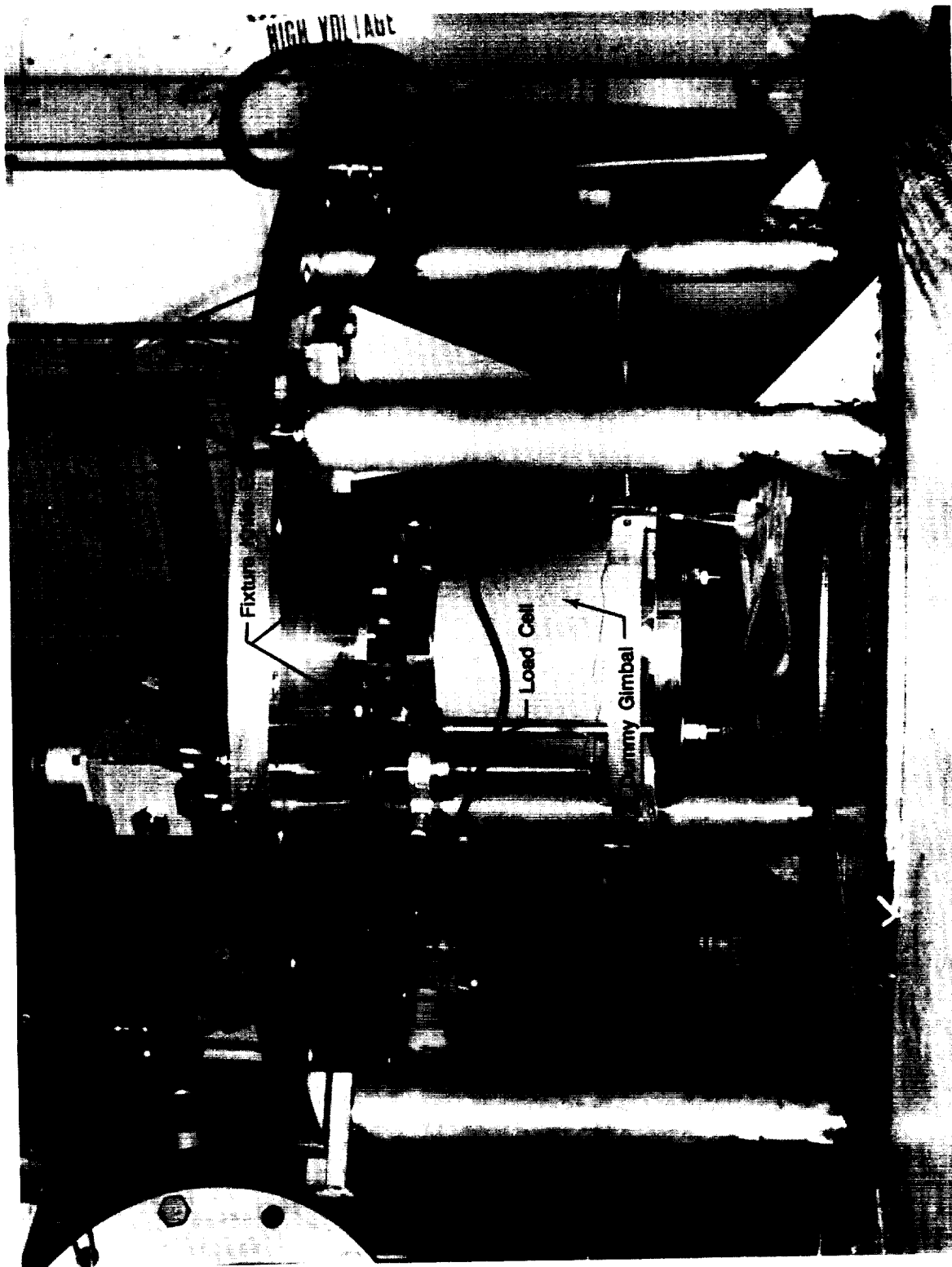
FD 320172

Figure 6. Atmospheric Side of Test Fixture (Insulation Not Shown)



NASA C-85-7724
FD 320173

Figure 7. Test Fixture Instrumentation



NASA C-85-6385

FD 320174

Figure 8. Dummy Gimbal Installed in Test Fixture

SECTION 3.0 FIXTURE SETUP AND INITIAL CHECKOUT

Complete instrumentation was provided with the test fixture. Full electronics to drive the gimbal rotation, and Vishay Strain Indicator/Switch and Balance units for strainage readings accompanied the rig. Thermocouples and load cells were provided in the fixture. NASA provided the Fluke Data-Logger, Honeywell O-graph, pre-amplifiers, amplifiers, and the digital data recorder.

Due to the joint nature of this effort, P&W did the design, assembly and test support of the gimbal fixture while NASA was responsible for facility support, test operations and data analysis. Prior to shipment of the fixture to NASA-LeRC, P&W checked out the operation of the fixture as far as practical using NASA supplied equipment. All data and testing discussed is presented in chronological order.

During initial checkout at LeRC, a problem was found with the design of the supply system to flow LN₂ into the test fixture. The planned approach was a gravity feed from a LN₂ supply tank four feet above the fixture. The pressure and flow of the LN₂ was not enough to overcome the ambient heat input even though the aluminum block and steel plate were insulated. NASA engineers reconfigured the LN₂ system to be a 25 psi forced flow system. This solved the temperature problem.

After 30 minutes of LN₂ flow, the temperature of the fixture cooling block decreased from 542°R (82°F) to 175°R (-285°F). When the rig was cooled to 160°R (-300°F) and the vacuum pulled, the bellows seal between the actuator and the interface began to leak. The bellows was removed, inspected, cleaned and reinstalled. The use of liquid Teflon helped seal the bellows and no more leaks occurred.

It was considered important to have clean hydraulic oil to avoid damaging the Moog valve. At first the stand was found to have oil that did not meet Moog valve cleanliness requirements. After many attempts to correct this problem, it was decided to test without the oil meeting the target specification level. The final conclusion was that the concern over oil quality was not totally justified, the reason being that the valve was to operate over a life much less than the valve design life.

Although load rod strain gages were calibrated during the fixture checkout at P&W, it was found necessary to have the strain gages calibrated on the low end of the strain gage scale (0 to 200 lb). The low end calibration was necessary so that the expected flight preload of approximately 100 lb could be applied during the gimbal testing. Also, as the fixture changed temperature, the calibration was used to reset that load which represented the expected flight engine load prior to vehicle deployment from the orbiter. The strain gages were calibrated by NASA technicians using a small hanging plate on which weights were added. The rods were low end calibrated at both ambient and cold temperatures while weights were hung in 10-lb increments and recorded, see Appendix A.

In addition to the calibration an investigation of the fixture cooldown rate and strain gage (thrust load cell changes) response to environmental changes was carried out. Figure 9 shows the load rods were near thermal equilibrium after a 24-hour soak. The mid-gimbal temperature trace confirmed that the gimbal reached equilibrium in a 24-hour period, also.

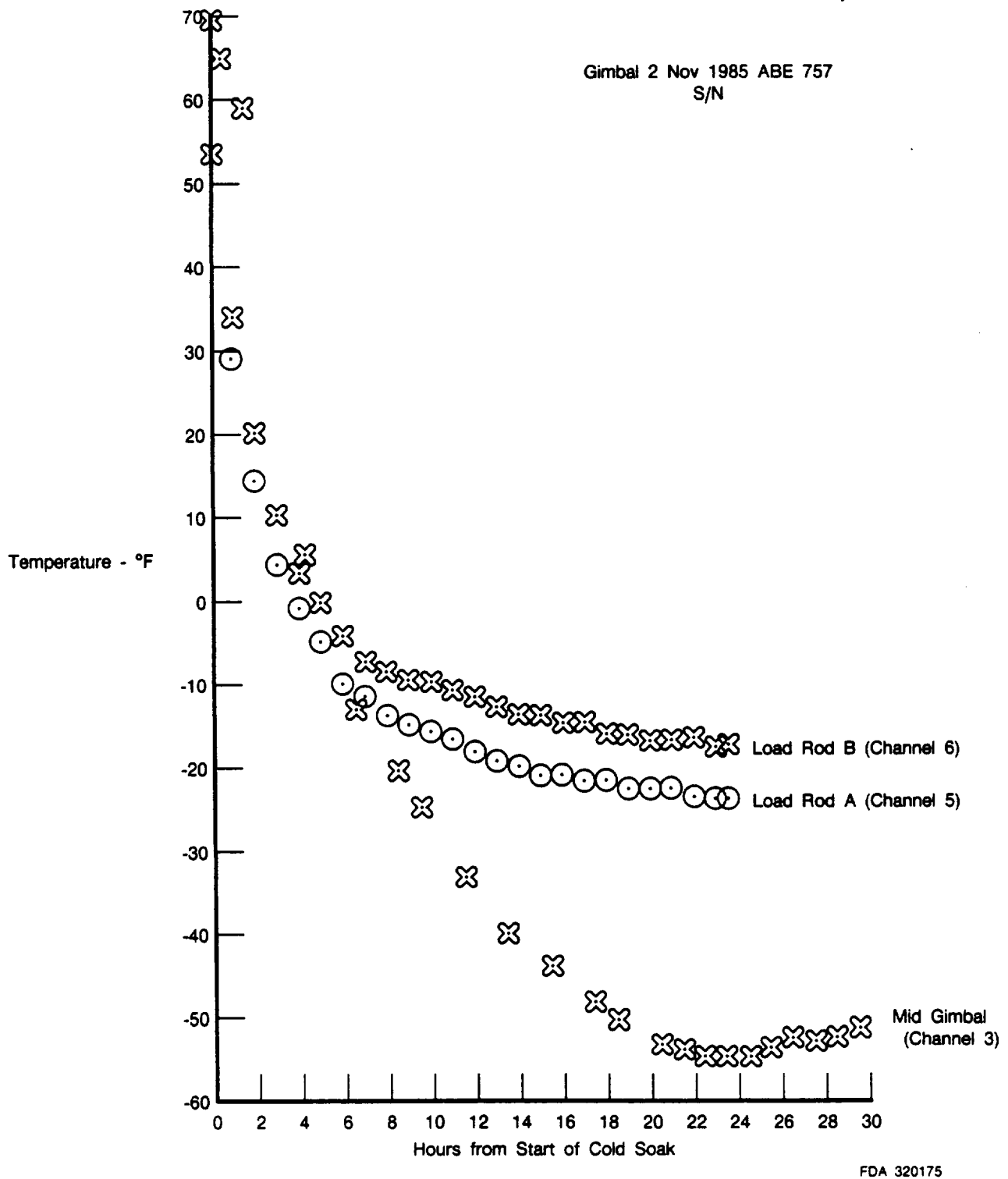
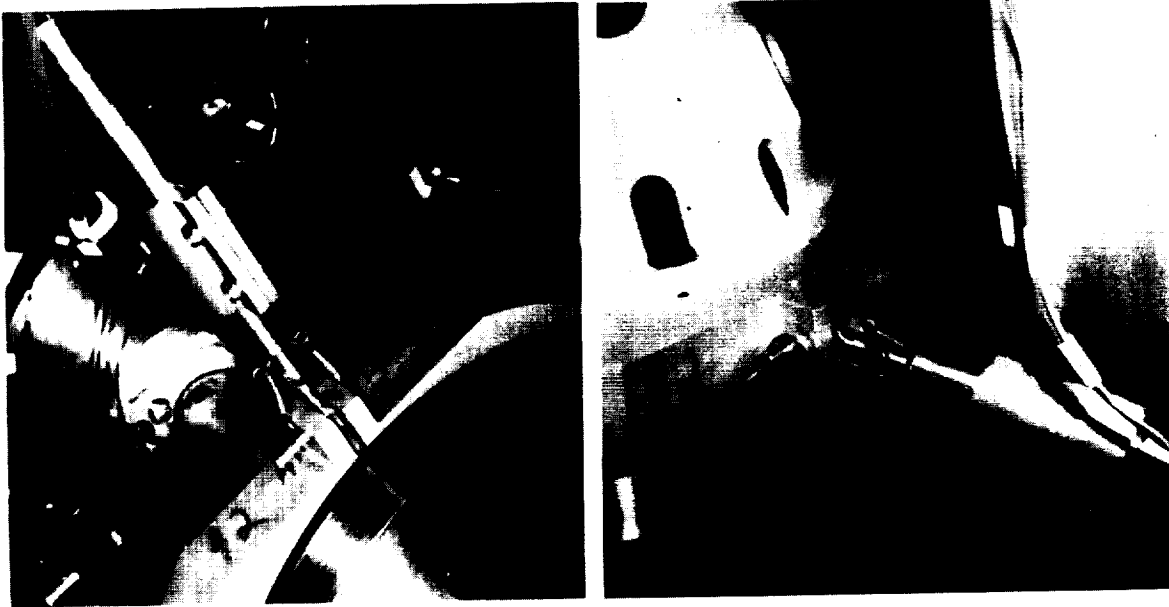


Figure 9. Cold Soak Temperature Data

The strain data tabulated from the hang tests and the thermal data were used to develop a preset load. This compensated for the ambient to cold strain gage shifts, weight of the fixture plates on the load rods, and a preload of 100 lb on the gimbal, simulating known prelaunch flight conditions.

During the checkout of the fixture with dummy and development gimbals, it was also discovered that as the gimbal moved, the key for the LVDT could jam from misalignment or friction between the key and key plate slot. This was fixed by NASA technicians who made and replaced the key with a universal joint key and spring system; the final configuration is shown in Figure 10.



FD 320176

Figure 10. Redesigned Key for LVDT

After the key problem was solved the load rod tightening of the two bellows plates was changed so that as one rod was tightened, the plates would not yaw out of alignment with the LVDT. The change made was to observe the LVDT key and tighten the plates so the key did not move. It was believed that this yaw might have contributed to the LVDT key problem.

After the key was replaced, it was found that the electronics continually tried to "hunt" for the right hydraulic valve setting. This was solved by reducing hydraulic pressure from approximately 1500 psi to 500 psi. The reduction of pressure did not affect response of the fixture or performance measurements.

Another problem was found with the fixture under vacuum and cold. A leak was found at the seal of the aluminum cooling block to the fixture plate. The leakage was eliminated by adding more bolts and torquing them after the fixture had cooled. When the fixture was cooled the bolts were torqued to 400 in.-lb before applying the simulated thrust load. This was done to eliminate the loss of the bolt preload applied to the aluminum cooling block after it cooled. The high torque was reversed after each test was completed so as not to overstress the bolts during the cooling block warming expansion.

SECTION 4.0 DEVELOPMENT TESTING

Three different gimbals were tested for friction levels and change of friction levels due to cycling. Gimbals with serial numbers ABE759 and BMC94 were tested in both pitch and yaw axes. Gimbal S/N ABE757 was tested in the pitch axis only. This gimbal was tested earlier at P&W during the fixture checkout. The gimbal was heat treated after original checkout to solve a stress corrosion cracking problem not associated with this testing. A retest of this axis was done to verify that the friction did not change after it was heat treated. In addition to checking the effects of the heat treat, the effect of having cracks was investigated since both development gimbals had stress corrosion cracks. No detrimental effect on gimbal performance was found. All three gimbals were tested to the test plan and test series shown in Table 2.

Table 2. Development Gimbal Test Plan

Conditions	Test Series	Number of Runs
0 Ambient Pressure and Ambient Temp	C	4
1 Vacuum and Cryo (Friction vs Cycles)	± 2 degrees @ 1Hz Sine	1
2 Vacuum and Cryo	A, B, C	12
3 Vacuum and Cryo and 1000 Cycles	C	4
4 Vacuum and Cryo and 2000 Cycles	C	4
5 Vacuum and Cryo and 4000 Cycles	C	4
6 Vacuum and Ambient Temp	C	4
7 Ambient Pressure and Ambient Temp	C	4

Test Points

Test Series	Waveform	Frequency Hz	Amplitude deg	Velocity deg/sec
A-1	Triangle	0.1	0.25	0.1
A-2	Triangle	0.5	0.25	0.5
A-3	Triangle	1.0	0.25	1.0
A-4	Triangle	2.0	0.25	2.0
B-1	Sine	0.1	0.25	0.157
B-2	Sine	0.5	0.25	0.785
B-3	Sine	1.0	0.25	1.571
B-4	Sine	2.0	0.25	3.142
C-1	Triangle	0.1	2.0	0.8
C-2	Triangle	0.5	2.0	4.0
C-3	Triangle	1.0	2.0	8.0
C-4	Triangle	2.0	2.0	16.0

Notes 1. All tests run at zero degree offset and 15,000 lb load.

0354C

As shown in Table 2, coulomb friction measurements were conducted at three different test conditions on gimbals ABE759 and BMC94: ambient temperature and pressure, ambient temperature and vacuum, and cryogenic temperature and vacuum. Measured gimbal coulomb friction levels are presented in Table 3. It can be seen that each change in the gimbal environment did change friction levels. Yet the changes were not as great for the 0.25 degree amplitude environments as the 2.00 degree amplitude environments.

Table 3. Friction Levels of Two Development Gimbals

<i>Test Condition</i>	<i>Gimbal Serial No.</i>	<i>Waveform</i>	<i>Frequency (Hz)</i>	<i>Amplitude (deg, 0-Peak)</i>	<i>Pitch Coulomb Friction (ft-lb, Peak-to-Peak)</i>	<i>Yaw Coulomb Friction (ft-lb, Peak-to-Peak)</i>	
Ambient Temperature and Pressure	ABE 759	Triangle	0.10	0.25	95.00	148.00	
			0.50		87.00	135.00	
			1.00		85.00	134.00	
			2.00		83.00	133.00	
	BMC 94	Triangle	0.10	2.00	92.00	83.00	
			0.50		90.00	75.00	
			1.00		86.00	61.00	
			2.00		81.00	53.00	
	Ambient Temperature and Vacuum	ABE 759	Triangle	0.10	2.00	64.00	136.00
				0.50		—	—
1.00				55.00		128.00	
2.00				54.00		127.00	
BMC 94		Triangle	0.10	2.00	58.00	63.00	
			0.50		63.00	58.00	
			1.00		65.00	55.00	
			2.00		63.00	50.00	
Cryogenic Temperature and Vacuum		ABE 759	Triangle	0.10	0.25	90.00	150.00
				0.50		85.00	148.00
	1.00			85.00		149.00	
	2.00			85.00		142.00	
	Sine		0.10	0.25	75.00	153.00	
			0.50		75.00	151.00	
			1.00		75.00	148.00	
			2.00		75.00	142.00	
	BMC 94	Triangle	0.10	2.00	25.00	93.00	
			0.50		30.00	75.00	
			1.00		35.00	73.00	
			2.00		35.00	72.00	
		Sine	0.10	0.25	83.00	57.00	
			0.50		76.00	50.00	
			1.00		72.00	50.00	
			2.00		72.00	47.00	
	Triangle		0.10	0.25	72.00	51.00	
			0.50		72.00	50.00	
			1.00		72.00	48.00	
			2.00		66.00	45.00	
		Triangle	0.10	2.00	43.00	11.00	
			0.50		44.00	10.00	
			1.00		42.00	10.00	
			2.00		45.00	9.00	

0354C

A three-day cold soak under vacuum was performed on gimbal ABE757 pitch axis to observe if 72 hours had any effect on gimbal friction; the temperature test data is shown in Appendix B. TCs show that the fixture and gimbal temperatures were stable after 24 hours and did not change significantly over the 24 to 72-hour time frame. The data recorded at 24 hours and 72 hours into the cold soak showed no difference in coulomb friction levels.

SECTION 5.0 PRODUCTION CYCLING

Based on the development testing which showed no significant change in torque after 15 cycles, it was decided to run 30 cycles on each production gimbal axis under simulated flight conditions. A summary of the cycles and torque levels for the production gimbals is shown in Figure 11. All data analysis was done by NASA LeRC and can be found in NASA Technical Memorandum 87335, September 86, Centaur Engine Gimbal Friction Characteristics Under Simulated Thrust Load, by James W. Askew (Appendix E). Gimbals BLE945 and BLE948 were selected as the flight gimbals because their torque levels were considered closest matched for the vehicle.

Gimbal Serial No.	Pitch Axis		Yaw Axis	
	Cycles	TB	Cycles	TB
BLE 945	32	57	30	56
BLE 948	30	48	51	58
BLE 962 (Spare)	30	42	51	60

Spring Constant K = ft-lb/deg
Torque TB = ft-lb

FD 320177

Figure 11. Data Summary of Production Gimbal Cycles and Friction Measurement

SECTION 6.0 CONCLUSIONS

A total of 32,000 cycles have been run on the development gimbal axes. Analysis of the cycle friction changes revealed that the first 10 to 15 cycles showed a small frictional level change after which there was no frictional level change over the entire cycle range tested (16,000 cycles on one axis). Conclusions drawn from the testing were:

- Environmental conditions affect torque levels to a small degree
- No changes in friction torque level occur past the first 15 cycles
- Coulomb friction levels were significantly lower (40 to 60 ft-lb for production gimbals) than the RL10A-3-3A design specification of 220 ft-lb
- Test fixture design and friction measurement performed to the expected design requirements.

SECTION 7.0
RECOMMENDATIONS

Test fixture design and testing showed that the fixture can be used further. Recommendations for continued investigation are:

- Use the fixture to correlate the effects of temperature and vacuum to ambient conditions so friction levels can be measured without vacuum and cold soak requirements
- Review engine vibration to determine, when vibration is added to the fixture, can it significantly affect the gimbal friction loads?

APPENDIX A
STRAIN GAGE CALIBRATION

Weight	$\mu \epsilon$ Ambient		$\mu \epsilon$ Cold	
	Channel 1	Channel 2	Channel 1	Channel 2
0	+00.00	+00.00	+00.00	+00.00
10	-6.1	-7.0	-6.5	-7.0
20	-9.1	-10.0	-10.0	-10.0
30	-12.4	-12.0	-12.0	-12.0
40	-14.3	-14.0	-15.5	-15.0
50	-17.0	-16.5	-18.2	-18.0
60	-19.5	-19.0	-21.0	-22.0
70	-22.5	-21.3	-24.5	-23.5
80	-25.1	-23.5	-28.0	-27.0
90	-28.0	-25.4	-30.5	-29.5
100	-30.9	-29.0	-32.9	-32.5
110	-32.5	-32.0	-36.0	-36.0
120	-36.5	-34.9	-39.0	-38.5
130	-38.5	-38.0	-42.0	-41.0
140	-42.0	-40.6	-44.5	-43.9
150	-44.0	-43.0	-47.5	-46.5
160	-46.5	-45.9	-50.5	-49.0
170	-49.0	-48.0	-53.5	-52.0
180	-52.0	-51.5	-56.0	-55.0
190	-54.5	-54.0	-58.5	-58.0
200	-57.0	-56.0	-61.5	-60.5
190	-55.0	-53.9	-59.0	-56.5
180	-52.0	-50.5	-56.0	-55.0
170	-49.0	-48.1	-54.0	-52.5
160	-47.0	-45.5	-51.5	-50.0
150	—	—	—	—
140	-40.0	—	-45.0	-44.0
130	—	—	—	—
120	-35.9	-34.5	-40.5	-38.0
110	—	—	—	—
100	—	—	-34.5	-34.0
90	—	—	—	—
80	-24.9	-22.5	-29.0	-28.0
70	—	—	—	—
60	—	-18.5	—	—
50	—	—	—	—
40	-14.8	-12.5	-19.5	-18.0
30	—	—	—	—
20	—	—	—	—
10	—	—	—	—
0	-00.00	+4.0	-7.5	-6.0

0134M

APPENDIX B
TC CHANNEL (°F)

Date/Time		TC #							
1985		0	1	2	3	4	5	6	7
Nov 1	0944	-299	-96	-141	5	-295	50	53	-15
	1044	-300	-114	-158	-4	-296	29	34	-24
	1144	-300	-124	-165	-13	-296	14	20	-33
	1244	-300	-130	-169	-20	-297	4	10	-39
	1344	-300	-133	-172	-25	-297	-1	3	-44
	1444	-300	-132	-170	-28	-296	-5	-0	-48
	1544	-300	-132	-169	-33	-296	-10	-4	-52
	1644	-301	-132	-170	-36	-298	-12	-7	-55
	1744	-301	-131	-169	-38	-298	-14	-8	-57
	1844	-301	-130	-168	-40	-298	-15	-9	-58
	1944	-301	-130	-168	-42	-298	-16	-10	-60
	2044	-301	-129	-167	-44	-297	-17	-11	-61
	2144	-301	-129	-167	-45	-297	-18	-12	-62
	2244	-301	-129	-167	-46	-297	-19	-13	-63
	2344	-301	-129	-167	-47	-297	-20	-14	-64
Nov 2	0044	-301	-129	-167	-48	-297	-21	-14	-65
	0144	-301	-129	-167	-49	-297	-21	-15	-66
	0244	-301	-130	-167	-49	-297	-22	-15	-66
	0344	-301	-130	-167	-50	-297	-22	-16	-67
	0444	-301	-130	-167	-50	-297	-23	-16	-67
	0544	-301	-130	-167	-51	-297	-23	-17	-68
	0644	-301	-130	-167	-51	-298	-23	-17	-68
	0744	-301	-130	-167	-52	-297	-24	-17	-68
	0844	-301	-130	-167	-52	-297	-24	-18	-69
	0957	-302	-130	-156	-58	-298	-25	-19	-79
	*1 1027	-302	-130	-155	-60	-298	-25	-20	-82
	*1 1057	-302	-131	-156	-62	-299	-26	-21	-83
	*1 1132	-302	-132	-150	-63	-299	-27	-22	-84
	*1 1245	-303	-134	-160	-66	-299	-30	-23	-87
	*1 1345	-301	-135	-172	-59	-289	-29	-22	-74
Nov 3	1445	-301	-133	-170	-57	-298	-28	-22	-72
	1545	-301	-131	-169	-56	-298	-27	-22	-72
	1645	-301	-130	-168	-55	-298	-27	-21	-71
	1745	-301	-130	-168	-54	-297	-26	-20	-70
	1845	-301	-129	-167	-54	-297	-26	-20	-70
	1945	-301	-129	-168	-54	-297	-25	-20	-70
	2045	-301	-129	-168	-53	-297	-25	-19	-69
	2145	-301	-130	-168	-53	-298	-25	-19	-69
	2245	-301	-130	-168	-53	-297	-25	-19	-69
	2345	-301	-130	-168	-53	-298	-25	-19	-69
	0045	-301	-130	-168	-53	-298	-25	-19	-69
	0145	-301	-130	-168	-53	-297	-25	-19	-69
	0245	-301	-130	-168	-53	-297	-24	-19	-69
	0345	-301	-130	-168	-53	-298	-24	-19	-69
	0445	-301	-130	-168	-53	-298	-24	-19	-69
	0545	-301	-130	-168	-53	-298	-24	-19	-69
	0645	-301	-130	-168	-53	-298	-24	-19	-69
	0745	-301	-130	-168	-53	-297	-24	-19	-69
	0845	-301	-130	-168	-52	-298	-24	-19	-69
	0945	-301	-130	-168	-52	-297	-24	-19	-69
	1045	-301	-129	-168	-52	-297	-24	-18	-69
	1145	-301	-129	-168	-52	-297	-24	-18	-68
	1245	-301	-129	-168	-52	-298	-24	-18	-68
	1345	-301	-129	-168	-52	-297	-24	-18	-68
	1445	-301	-129	-168	-52	-297	-24	-18	-68
	1545	-301	-129	-168	-52	-297	-24	-18	-68
	1645	-301	-129	-168	-52	-297	-24	-18	-68

Appendix B. TC Channel (°F) (Continued)

Date/Time		TC #							
1985	0	1	2	3	4	5	6	7	
	1745	-301	-129	-168	-52	-297	-24	-18	-68
	1845	-301	-129	-168	-52	-297	-24	-18	-68
	1945	-301	-129	-168	-52	-297	-24	-18	-68
	2045	-301	-129	-168	-52	-297	-24	-18	-68
	2145	-301	-129	-168	-52	-297	-24	-18	-68
	2245	-301	-129	-168	-52	-298	-24	-18	-69
	2345	-301	-129	-168	-52	-297	-24	-18	-69
Nov 4	0045	-301	-129	-168	-52	-298	-24	-18	-69
	0145	-301	-129	-168	-52	-297	-24	-18	-69
	0245	-301	-129	-168	-53	-298	-24	-18	-69
	0345	-301	-129	-168	-53	-298	-24	-18	-69
	0445	-301	-129	-168	-52	-297	-24	-18	-69
	0545	-301	-129	-168	-53	-297	-24	-18	-69
	0645	-301	-129	-168	-53	-298	-24	-18	-69
	0745	-301	-129	-168	-53	-298	-24	-18	-69
	0845	-301	-129	-168	-53	-298	-24	-18	-69
	0945	-301	-129	-167	-52	-298	-24	-18	-69
*2	1037	-301	-129	-167	-52	-298	-24	-18	-69
	1045	-301	-130	-159	-55	-297	-24	-18	-76
*3	1053	-299	-129	-156	-56	-294	-24	-18	-77
*4	1111	-298	-129	-154	-57	-294	-24	-18	-78
	1115	-298	-129	-154	-57	-294	-24	-18	-78
*5	1119	-301	-128	-154	-58	-297	-24	-19	-78
	1138	-302	-129	-154	-60	-299	-25	-19	-81
	1145	-268	-129	-163	-58	-267	-25	-19	-75
	1215	-26	-40	-44	-32	-26	-23	-18	—
	1245	+54	+39	+40	-4	+54	-17	-12	+0
	1315	74	66	66	12	73	-3	-0	—
	1345	75	72	74	25	75	12	13	29
	1345	75	72	74	26	75	12	14	—
	1346	74	72	74	34	74	19	20	34
	1347	74	72	74	36	74	23	23	36
	1349	74	72	74	40	74	32	31	41
	1350	74	72	74	42	74	36	36	43
	1403	73	72	73	53	73	53	54	54
	1415	74	74	76	70	75	69	69	—
	1420	75	76	78	85	76	78	83	75
	1425	76	76	78	87	77	81	85	85
*6	1438	76	76	77	79	77	79	79	79
	1445	77	76	77	78	77	79	79	78

*1 — 4 hr test series taken here

*2 — 2 hr test series started

*3 — 2500 cycles reached

*4 — 8000 cycles reached

*5 — 10,000 cycles reached, end testing of 72 hr soak

*6 — Baseline amb temp and no vacuum test

0134M

APPENDIX C
REFERENCE MEMOS

REFERENCE 1

PRATT & WHITNEY
Engineering Division South

INTERNAL CORRESPONDENCE

To: W. B. Lunn
From: S. L. Imbrogno
Subject: RL-10 Gimbel Mount Test Rig Force Measurement Uncertainty
Date: April 10, 1985
Copy To: M. Calandra, R. H. Dieck, A. Palgon, I.V. File.

SUMMARY:

Applied force uncertainty for the RL-10 gimbel mount test rig was compared for two different measurement methods. Method 1 measures the amount of pressure applied to the load generating metal bellows and calculates applied force using the bellows area and measured pressure. Method 2 measures the strain in two vertical rig support rods and relates the measured strain to applied force on the gimbel mount.

The uncertainty in applied force using Method 1 was calculated to be ± 40.5 lbs or $\pm 0.27\%$ at 15000 lbs. applied load. This value assumes that two $\pm 0.25\%$ "orange band" pressure transducers are averaged to measure bellows pressure. Uncertainty in bellows diameter is assumed to be ± 0.001 in. Uncertainty in applied force using Method 2 was calculated to be ± 375 lbs. or $\pm 2.5\%$ at 15000 lbs. applied load. This assumes strain gaged support rods are calibrated at cryogenic temperatures. A summary of of these results appear in Table 1.

RECOMMENDATIONS:

Force applied to the RL-10 gimbel by the test rig may best be determined by measuring bellows pressure (averaging two $1/4\%$ uncertainty pressure transducers) and area and calculating the resultant force generated by the bellows. Direct measurement of force using strain gaged support rods require that the strain gaged support rods be calibrated at cryogenic temperatures. This type of calibration is currently not available at GPD.

W. B. Lunn

- 2 -

April 10, 1985

TABLE 1.
Uncertainty in calculated gimbel mount applied load

MEASUREMENT METHOD	BIAS	PRECISION t95 S	UNCERT.
Pressure x area w/ 0.6% transducer	+/-0.38%	+/-0.38%	+/-0.76%
w/ 1/4% transducers two averaged	+/-0.16%	+/-0.11%	+/-0.27%
one transducer	+/-0.16%	+/-0.16%	+/-0.32%
Strain-gaged supports*	+/-2%	+/-0.5%	+/-2.5%

*Assumes gage calibrated at cryogenic temperature on supports.



S. L. Imbrogno, Ext. 3800
Instrument Validity/Integrity

SLI:sli

REFERENCE 2

PRATT & WHITNEY
Engineering Division South

INTERNAL CORRESPONDENCE

To: M. Calandra
From: S. L. Imbrogno
Subject: RL-10 Gimbel Friction Test Pre-test Uncertainty Analysis
Date: May 21, 1985
Copy To: Dr. R. B. Abernethy, R. H. Dieck, W. B. Lunn, E. A. Pinsley,
I.V. File.

Reference: Ref. 1, Static and Dynamic Characteristics of
Centaur Gimbel System Under Thrust Load, R. J.
Antl et al, NASA LeRC, not dated.

Ref. 2, AEDC-TR-73-5 Handbook, Uncertainty in
Gas Turbine Measurements, Dr. R. B. Abernethy et
al, 2/1973

HIGHLIGHTS:

- o Based on published specifications for the Straincert load cell and the Schaevitz Engineering LVDT, (linear displacement transducer), the uncertainty of the Coulomb friction for the RL-10 gimbel mount would be ± 40.4 in-lbs or 10.3%
- o Assuming in-house calibration of the load cell in the 0 to 300 lbs. range demonstrates improved load cell performance, as expected, Coulomb friction uncertainty would be ± 17.1 in-lbs or 4.4%, thus meeting the project goal of $< \pm 5\%$ uncertainty.

DISCUSSION:

Measurement uncertainty was estimated for RL-10 Gimble friction tests. Gimbel friction will be determined by rotating an RL-10 gimble in a test rig and measuring the force required to rotate the rig at various angular velocities. Force measurement will be made using a load cell mounted in the drive push rod. Angular velocity will be measured by determining the time required for the gimbel to move thru a $\pm .25$ deg. arc. A LVDT will sense gimbel movement.

M. Calandra

- 2 -

May 21, 1985

Ref. 1 defines friction torque as:

$$T_f = B_r \dot{\delta} + B_c \dot{\delta} / |\dot{\delta}| \quad \text{or}$$

$$T_f = B_r \dot{\delta} \pm B_c.$$

where T_f = measured friction torque, in-lbs,
= measured load x distance from gimbel pin
to drive pin.
= $F_m \times D$

B_r = viscous friction, in-lbs,

$\dot{\delta}$ = rig angular velocity, deg./sec.

B_c = coulomb friction, in-lbs.

δ may be defined as:

$$\delta = (L/R * 57.3) * \omega \cos \omega t$$

where L = measured displacement of gimbel rig,
(output of LVDT in inches).

R = vertical distance from gimbel bearing
centerline to LVDT mounting pin centerline.

$\omega = 2 \pi f$, where f is the frequency of gimble motion.

t = time for 1 cycle.

Viscous friction is determined by plotting friction torque vs. angular velocity for various angular velocities from 0.0625 deg./sec. to 8.00 deg./sec. and finding a best fit straight line connecting the points. The slope of this line is defined as "viscous friction" and the intercept is defined as "coulomb friction".

Uncertainty in viscous friction was estimated by error propagation thru the formula:

$$B_r = \overline{T_f} / \overline{\dot{\delta}}$$

Coulomb friction uncertainty was estimated by propagation of measured friction torque and measured angular velocity uncertainties by the Taylor series method of Ref. 2. The equation used for this propagation is obtained by rearranging terms in the above equations to obtain:

$$B_c = F_m * D - B_r(L/R * 57.3) * \omega \cos \omega t.$$

Nominal values and related uncertainties are listed in Table. 1.

M. Calandra

- 3 -

May 21, 1985

TABLE 1
NOMINAL VALUES AND RELATED BIAS AND PRECISION ERRORS.

Case 1 Data			
PARAMETER	NOMINAL VALUE	+ - BIAS ERROR	+ - PRECISION ERROR
Fm	60.0 lbs.	1.41 lbs.	1.16 lbs.
D	10.78 in.	0.003 in.	N/A
Br	31.92 in-lbs	2.74 in-lbs.	N/A
L	0.0391 in.	0.0012 in.	neg.
ω	32.00 rad/sec.	neg.	neg.
t	0.196 sec.	neg.	neg.
R	8.957 in.	0.003	N/A

Case 2 Data			
PARAMETER	NOMINAL VALUE	+ - BIAS ERROR	+ - PRECISION ERROR
Fm	60.0 lbs.	0.42 lbs.	0.35 lbs.
D	10.78 in.	0.003 in.	N/A
Br	31.92 in-lbs	1.23 in-lbs.	N/A
L	0.0391 in.	0.0012 in.	neg.
ω	32.00 rad/sec.	neg.	neg.
t	0.196 sec.	neg.	neg.
R	8.957 in.	0.003	N/A

Case 1 refers to the estimate assuming manufacturer specified load cell performance. Case 2 refers to improved load cell performance because of in-house calibration to 300 lbs. full scale.

Estimated uncertainty for coulomb friction is shown in Table 2.

TABLE 2
COULOMB FRICTION UNCERTAINTY

CASE	+ -BIAS		+ -PRECISION		+ -UNCERTAINTY	
	in-lbs	%	in-lbs	%	in-lbs	%
1	27.87	7.1	12.5	3.2	40.37	10.3
2	13.38	3.4	3.77	0.96	17.15	4.38

Contribution of uncertainty in measured parameter to uncertainty in coulomb friction is shown in Table 3.

M. Calandra

- 4 -

May 21, 1985

TABLE 3
UNCERTAINTY IN COULOMB FRICTION DUE TO INPUT PARAMETER
IN UNITS OF IN.-LBS.

CASE 1

PARAMETER	INF. COEF.	BIAS	PREC.	UNCERT.
Fm	10.78	15.20	12.50	27.70
Br	8.00	22.01	N/A	22.01
L	6533.71	7.8	neg.	7.8
D	59.98	0.18	N/A	0.18
R	28.52	0.09	N/A	0.09
RSS		27.87	12.50	40.37

CASE 2

PARAMETER	INF. COEF.	BIAS	PREC.	UNCERT.
Fm	10.78	4.53	3.77	8.3
Br	8.00	9.84	N/A	9.84
L	6533.71	7.8	neg.	7.8
D	59.98	0.18	N/A	0.18
R	28.52	0.09	N/A	0.09
RSS		13.38	3.77	17.15

RECOMMENDATIONS:

Based on this pre-test uncertainty analysis, it is recommended that the load cell used to measure gimble friction force be calibrated, in-house, for 0 to 300 lb. full scale.



S. L. Imbrogno, Ext. 3800
Instrument Validity/Integrity

SLI:slj

C-7

REFERENCE 3

PRATT & WHITNEY CONTROLLED

DESIGN SUBSTANTIATION MEMO

ENGINE MODEL RL10		AREA CODE 42 72 000 000	LAYOUT NO. L-240212	YR 85	SERIES 711	JOB NO. A0600S
				DATE June 5, 1985		

SUBJECT:

GIMBAL FRICTION TEST FIXTURE

DISTRIBUTION: M. Calandra

T. Kmiec

W. Ring

W. Sheltz

SUMMARY:

A specific Shuttle-Centaur mission requires that the force to gimbal the engine due to the friction within the gimbal's spider pins be determined. This data is required for input into the vehicle's guidance programming in order to obtain an accurate payload orbit.

A test fixture has been designed to measure the gimbal frictional forces under simulated engine thrust load and in a vacuum and temperature controlled environment. This fixture has been designed to be used in the Lewis Research Center (NASA) large bell jar vacuum chamber.

DISCUSSION

The test fixture is mounted on a 40 in. diameter steel plate, which also forms the end closure of the cylindrical vacuum chamber. The fixture permits the gimbal to rotate a maximum of ± 2.25 degrees, while under a simulated 15,000 lb. thrust load from a pneumatic actuator. A Moog actuator was chosen to rotate the gimbal at which the tests will be performed at gimbal positions of null, ± 1 & ± 2 degrees. The gimbal will be oscillated about each of these positions at an amplitude of $\pm .25$ degrees ($\approx \pm .027$ in. actuator displacement) at frequencies varying from .04 to 5 Hz. A Strainert load cell is incorporated into the actuation rod in order to record the load required to move the gimbal. This load value will be used to calculate the gimbal frictional force. An aluminum cooling block, to which the gimbal is mounted, contains passages through which LN2 will flow to maintain the gimbal mount temperature at approximately 175°R. This is to simulate the gimbals proximity to the vehicle's lox tank. Thermocouples will be installed at several locations (specified by Project Engineering) in order to monitor the temperature of the gimbal and fixture.

PREPARED BY <i>A. M. Palgon</i> A. M. Palgon	APPROVED BY <i>J. F. Marshall</i> J. F. Marshall	APPROVED BY
----------------------------------------------------	--------------------------------------------------------	-------------

This document is the property of United Technologies Corporation and is delivered on the express condition that it is not to be disclosed, reproduced in whole or part, or used for manufacture for anyone other than United Technologies Corporation without its written consent; and that no right is granted to disclose or to use any information contained in said document. This restriction does not limit the right to use information obtained from another source.

PRATT & WHITNEY CONTROLLED

-2-

YR	SERIES	JOB NO.
85	711	A0600S

Knife edges (.040R point) are used as the pivoting point in order to obtain and minimize fixture friction. A dummy gimbal was designed with a set of knife edges to operate the test fixture and measure the knife edge friction so this load, along with the fixture's inertial loads, can be subtracted out from the recorded actuation load during test operation. The hydraulic actuator contains a LVDT for indicating linear displacement and a LVDT has been mounted adjacent to the gimbal plate to record actual gimbal displacement corresponding to gimbal angular rotation.

CONCLUSION:

Careful assembly, alignment and calibration of the test fixture will generate the most accurate gimbal frictional loads that can be measured.

REFERENCES:

- 1) Memo, "RL10 Gimbal Mount Test Rig Force Measurement Uncertainty", S. L. Imbrogno to W. B. Lunn, 4/10/85.
DGVO, "RL10 Gimbal Test", T. Swartwout to A. Palgon, 4/16/85.
- 3) Memo, "RL10 Gimbal Friction Test Rig Design Review", R. J. Ryberg to M. C. Calandra, 4/18/85.

AMPms

This document is the property of United Technologies Corporation and is delivered on the express condition that it is not to be disclosed, reproduced in whole or part, or used for manufacture for anyone other than United Technologies Corporation without its written consent; and that no right is granted to disclose or to use any information contained in said document. This restriction does not limit the right to use information obtained from another source.

REFERENCE 4

PRATT & WHITNEY
Engineering Division South

INTERNAL CORRESPONDENCE

51080014

To: M. C. Calandra
From: R. J. Ryberg
Subject: RL10 Gimbal Friction Test Rig
Design Review
Date: April 18, 1985
Copy To: G. Leddy, Participants

1. The review was held on 17 April 1985 with participants as listed on the attached sheet. A simplified schematic of the rig is attached. The concept appeared satisfactory, however, there were many items identified for additional study and consideration.
2. The pertinent comments and recommendations are as follows:
 - a) The gimbal actuators are 90° apart and in line with the gimbal universal joints. The rig has to have gimbal thrust load rods ($2-180^{\circ}$ apart) are in line with the gimbal rotating axis which only allows the use of a single actuator. Tests should be run with the actuator in line with a universal joint axis and half way between the universals axes to determine if there is a variability in friction. This will determine if all the tests can be run with the actuator in one location.
 - b) Vibration data from engine testing should be reviewed and a test run with realistic vibration to determine if it can significantly effect the gimbal friction loads.
 - c) The loading rods have to pivot or bend at a location in line with the gimbal universal axis. A balance scale pivot or a bending flexure were studied. The flexure would not be effected by wear and is less likely to effect measured friction forces. The following comments were generated:
 1. The flexure would be preferrable if the necessary flexibility can be obtained with adequate strength margin.
 2. The flexure cross section may have to be tapered to focus the bending location and to provide better stress distribution.

M. C. Calandra

- 2 -

April 18, 1965

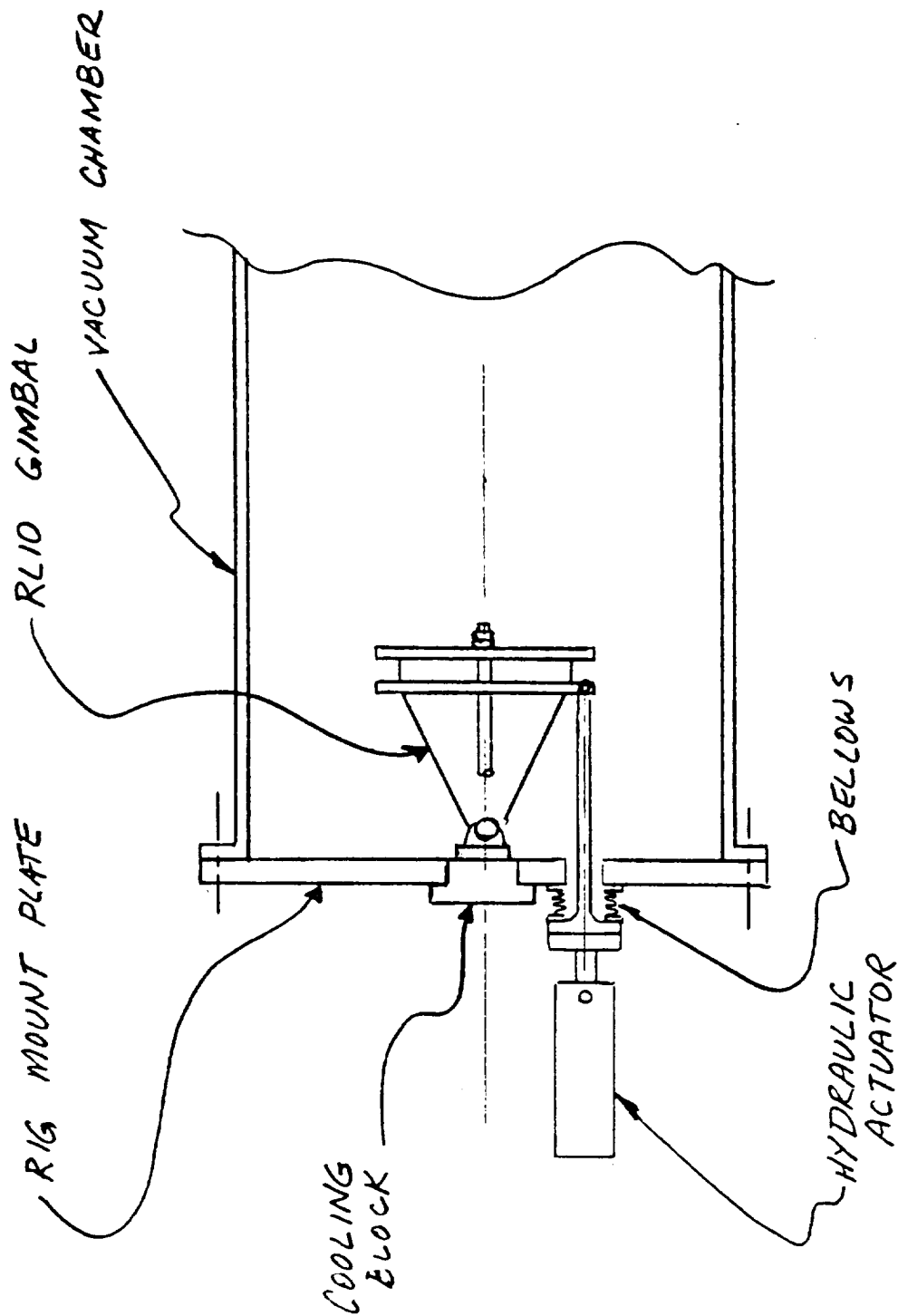
3. Depending on the material used for the flexure, it may be desirable to eddy current inspect these to minimize the flaw size.
 4. The flexures or pivots will have to be calibrated for effects on measured friction loads.
 5. The load rods should have a minimum safe cross section to allow bending for alignment without effecting friction loads being measured.
 6. The load actuator is pneumatic and requires air pressures up to 200 PSI. The amount of stored energy and the reaction on the freed mass if a flexure fails should be reviewed and a catcher provided if necessary.
- d) The vacuum chamber cover and rig mounting plate deflection due to gimbal thrust load and vacuum ΔP may have to be taken into account.
 - e) The materials of the chamber cover, etc. may not have to be stainless, but have to have the vacuum side surfaces cleanable to minimize outgasing problems.
 - f) The gimbal load actuator should have a pressure limiter so the system cannot be inadvertently overloaded.
3. Mr. M. Calandra is responsible for ensuring action follow-ups of the above and documenting the action response.



R. J. Ryberg, Ext. 5173
Chief Engineer's Office

RJR:haf

ATTACHMENT



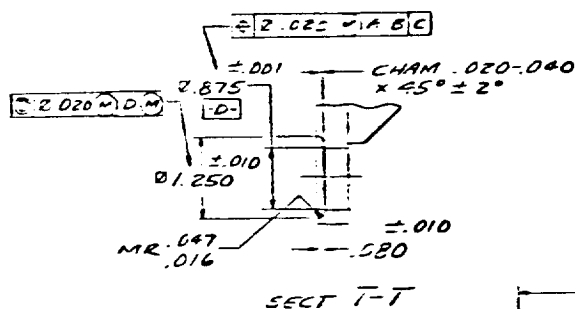
APPENDIX D
GIMBAL TEST FIXTURE DRAWINGS

The layout prints are not current to the fixture in the areas of:

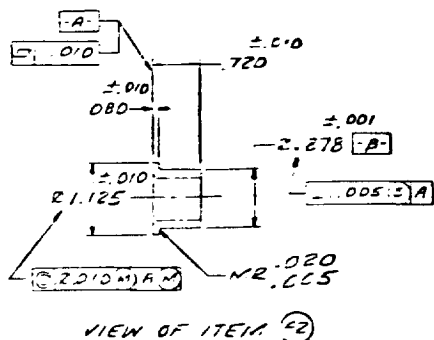
1. A Strainert load cell was added to the actuator rod on the vacuum side of the plate.
2. Item 13 was changed to 347 stainless steel.
3. Item 17 was redesigned to allow additional flexure of the bellows.
4. Item 27 had additional bolts added to hold down the cooling block.
5. LVDT key Item 46 was redesigned as shown in Figure 10. (See Section 3)

	1	71	SH 3	HOUSING	AMS 347 SST		NSQR
	1	70	SH 3	BLADE	AMS 5845 CO ALLOY	NOTE 22	NSQR
	1	69	SH 3	BLADE	AMS 5845 CO ALLOY	NOTE 22	NSQR
	1	68	SH 3	HOUSING	AISI 347 SST		NSQR
	1	67	SH 2	CLAMP	AISI 347 SST		NSQR
	1	66	SH 2	PLATE		.250 X .010 THICK	NSQR
	1	65	SH 2	PLATE		.250 X .010 THICK	NSQR
	1	64	SH 2	PLATE		.500 X .010 THICK	NSQR
	X	163	SH 2	BACKET-ASST OF	AISI 347 SST	NOTE	NSQR
		162		ACTUATOR		NOTE 18	
	1	61		MS 2336-B1 'O' RING	AMS 7267		
	8	60		MS 2420-10 BOLT	AMS 5731 SST	.250-28 UNF-3A LENGTH .750	
	1	59	SH 2	COUPLING	AISI 347 SST		NSQR
	8	58		MS 2498-22 SCREW	ALLOY STEEL	.190-32 .625 LONG	
	1	57		MS 2525-26 PIN	AMS 5616 SST	.2454-.24400 = .1640 LONG	
	3	56		MS 2591-20 BOLT	AMS 5731 SST	.3125-24 UNF-3A LENGTH 1.500	
	4	55		MS 2591-10 BOLT	AMS 5731 SST	.3125-24 UNF-3A LENGTH .875	
	1	54		COUPLING-FLEXIBLE		NOTE 17	
	1	53		ROD END	SST	NOTE 16	
	1	52		MS 2361-12 NUT-JAM	AMS 5725 OR 5727	.375-24 UNF-3B	
	1	51	SH 2	FLANGE	AISI 347 SST		NSQR
	1	50	SH 2	ROD	AISI 347 SST		NSQR
	X	149	SH 2	ROD-ASST OF			NSQR
	63142	1	Q	Q	Q	Q	Q
	Q	Q	Q	Q	Q	Q	Q

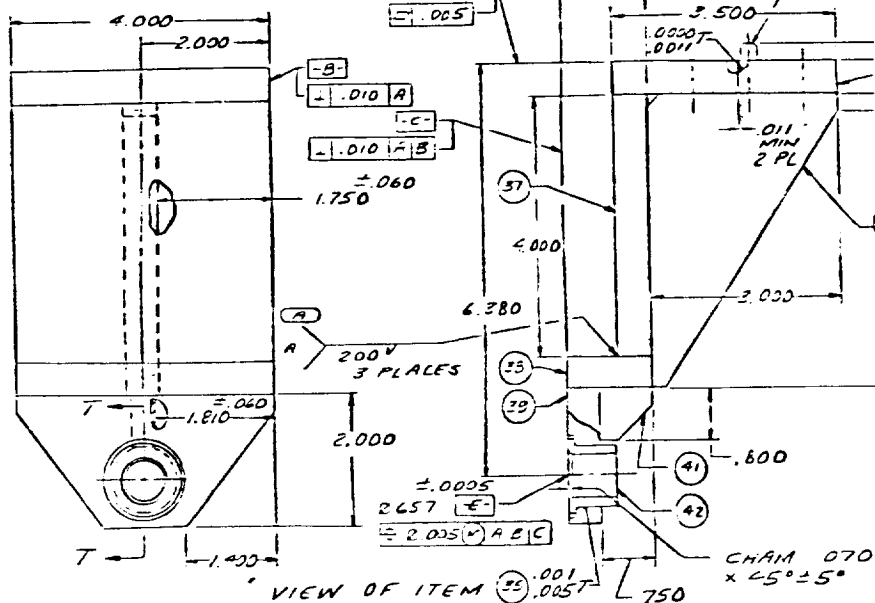
LAYOUT FOLLOW-UP LIST



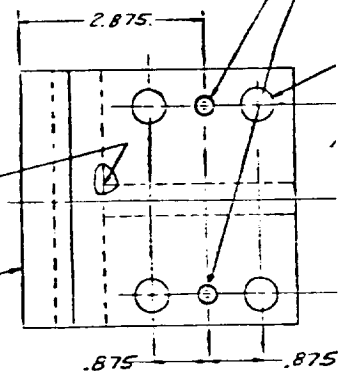
SECT T-T



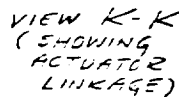
VIEW OF ITEM ②



VIEW OF ITEM ③

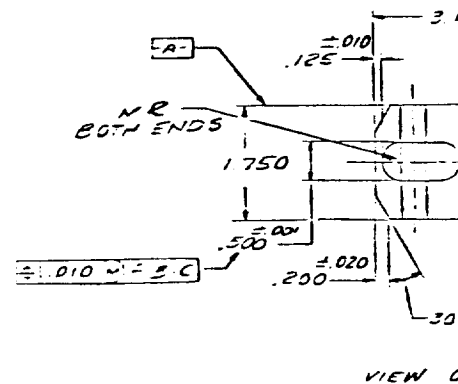
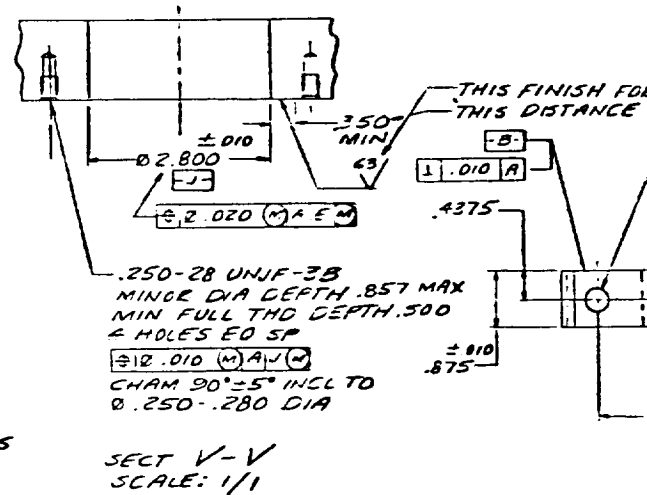
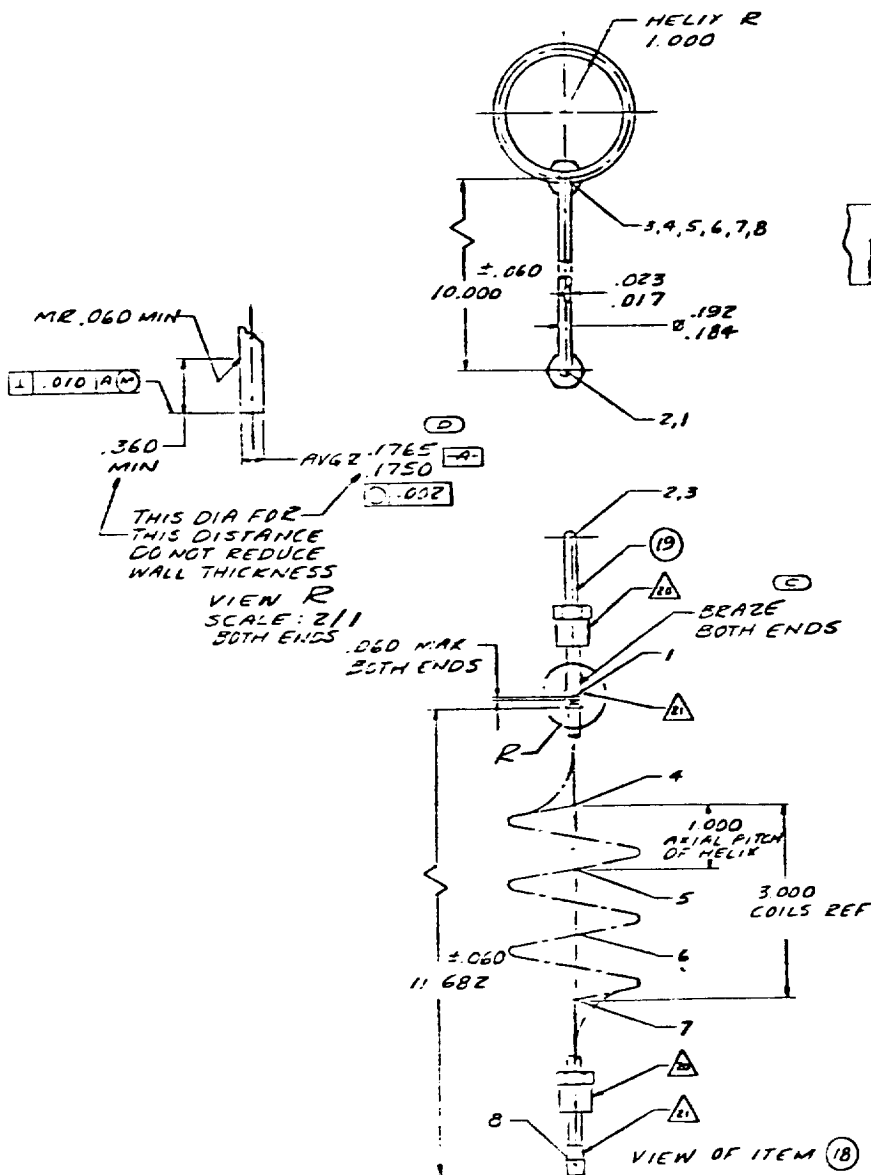


2.875 ± .001
2.875 ± .001
2.875 ± .001

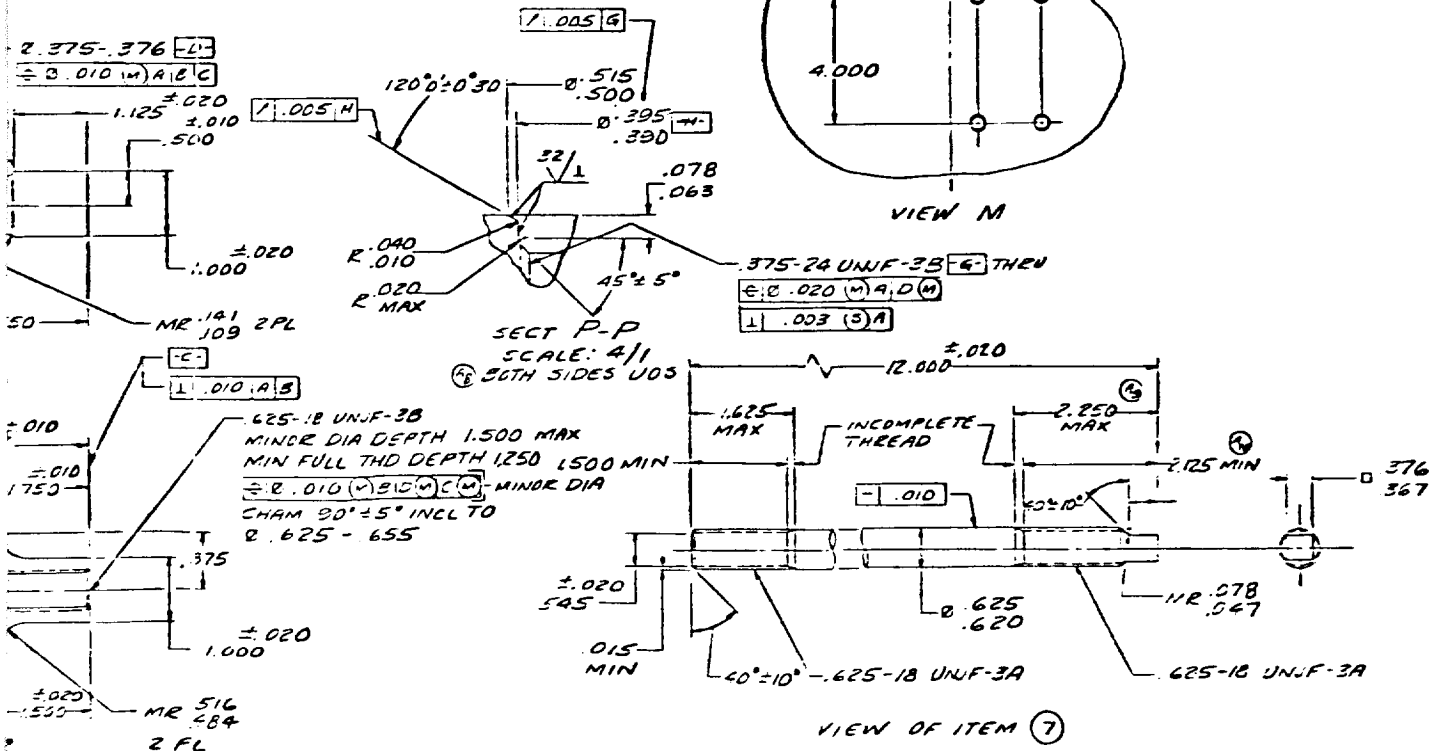
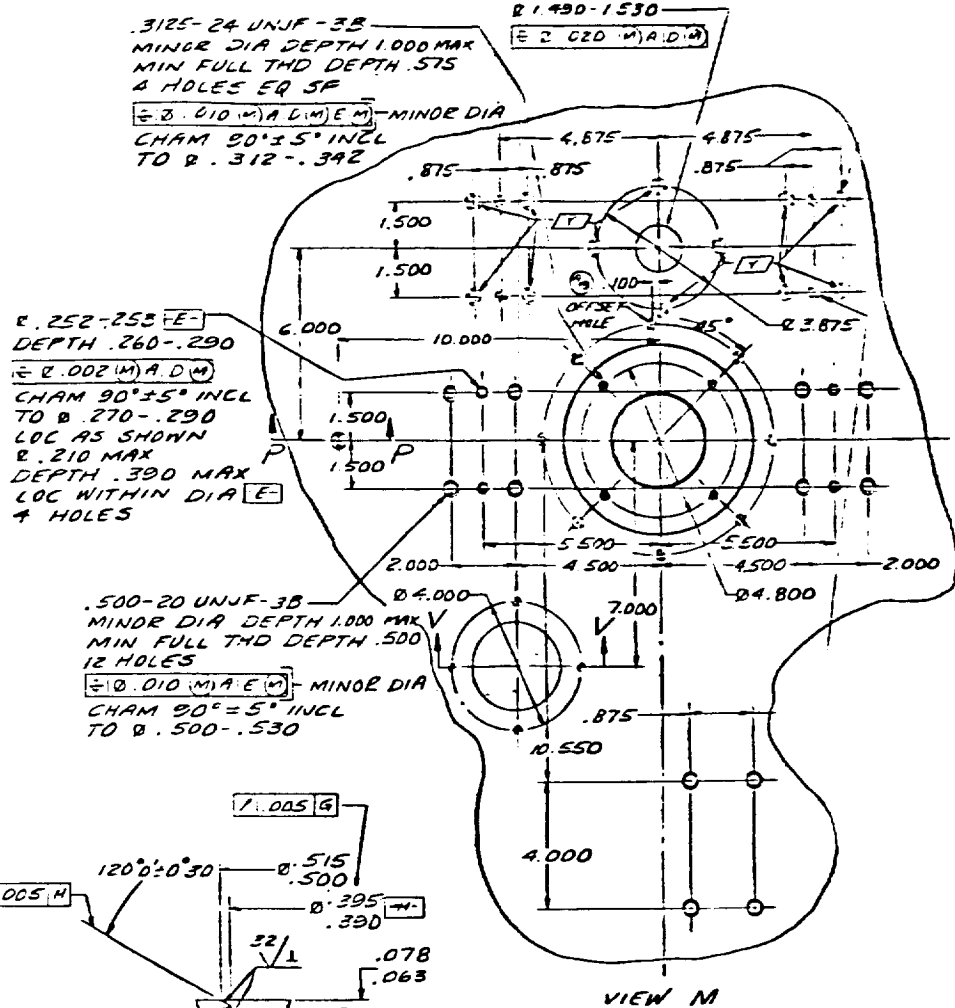


19 LOCATION OF TUBE POINTS				
FROM PT. 1 TO	X	Y	Z	RADIUS
2	.000	.000	3.500	1.000
3	.000	.000	3.500	1.000
4	.000	10.000	-6.000	SEE VIEW
5	.000	10.000	-7.000	SEE VIEW
6	.000	10.000	-8.000	SEE VIEW
7	.000	10.000	-9.000	1.000
8	.000	10.000	-11.682	—
TOL BETWEEN END POINTS = .060				

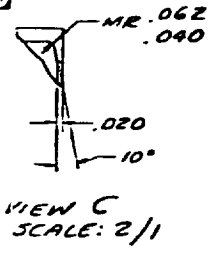
19 DEVELOPED LENGTH 3.2				
TRUE LENGTH OF STRAIGHT ALONG LINE	A	B REF	ANGLE OF TWIST (REF)	BEND (N TO ADJAC LOC
1-2	2.500	—	—	2
2-3	—	8.000	1.4 3.2 90° CW	3
3-4	—	7.500	HELIX	4
4-5	—	—	HELIX	5
5-6	—	—	HELIX	6
6-7	—	—	HELIX	7
7-8	1.682	—	—	—

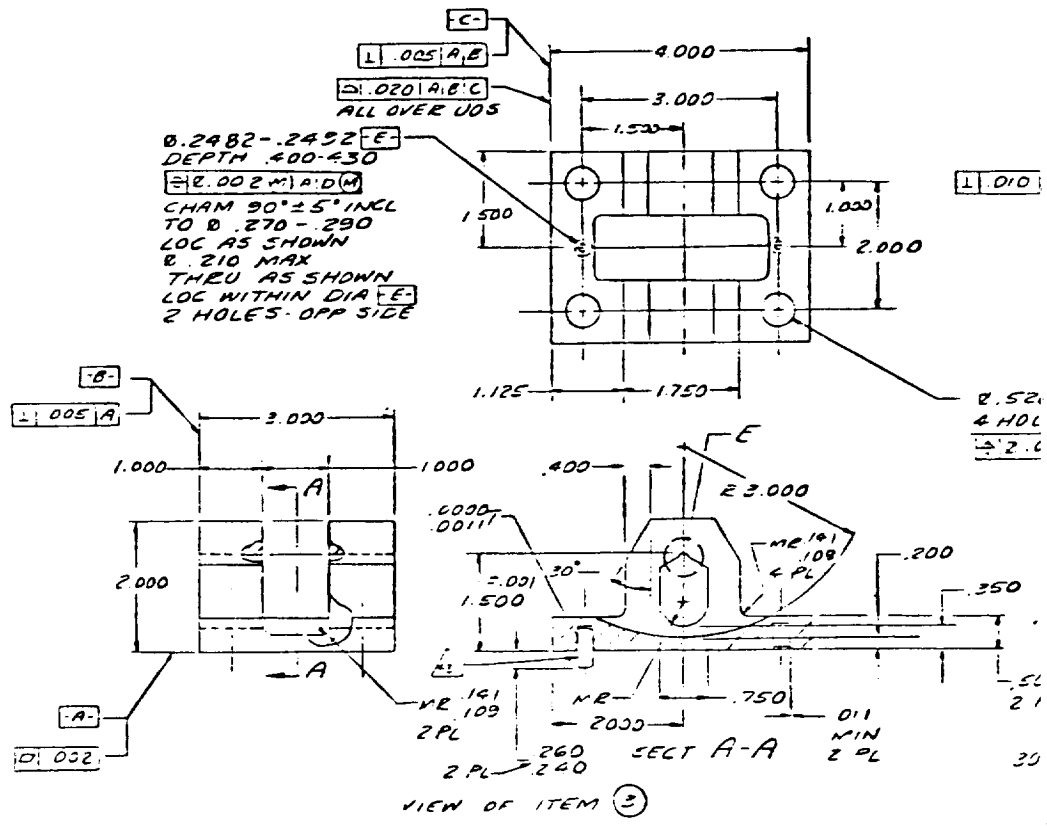
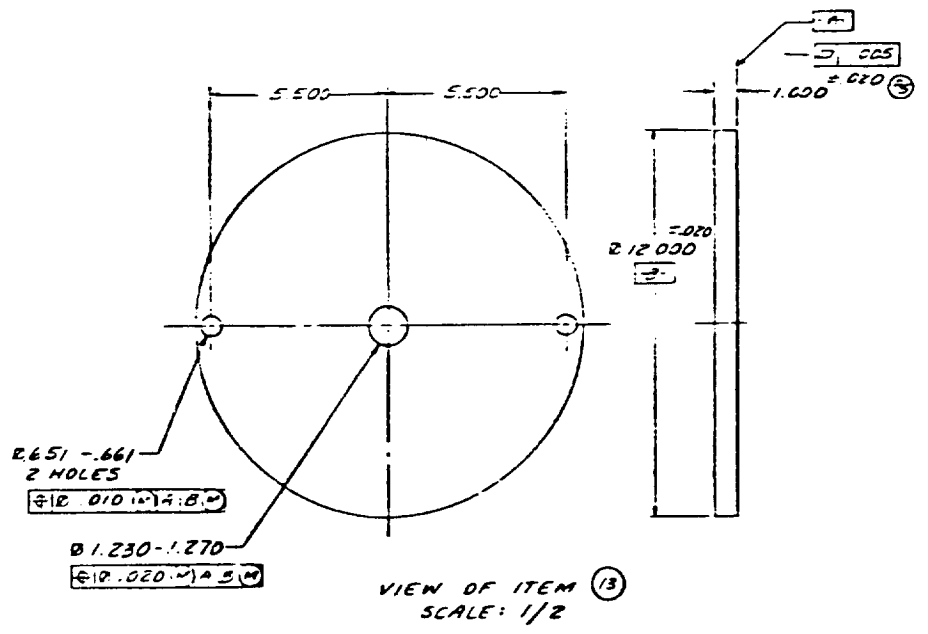


60 REF			
NE COMMON	T	REF	
STRAIGHTS			
US			
REF			
00	90°	1.000	
00	90°	1.000	
00	—	—	
00	—	—	
00	—	—	
00	—	—	
00	—	—	



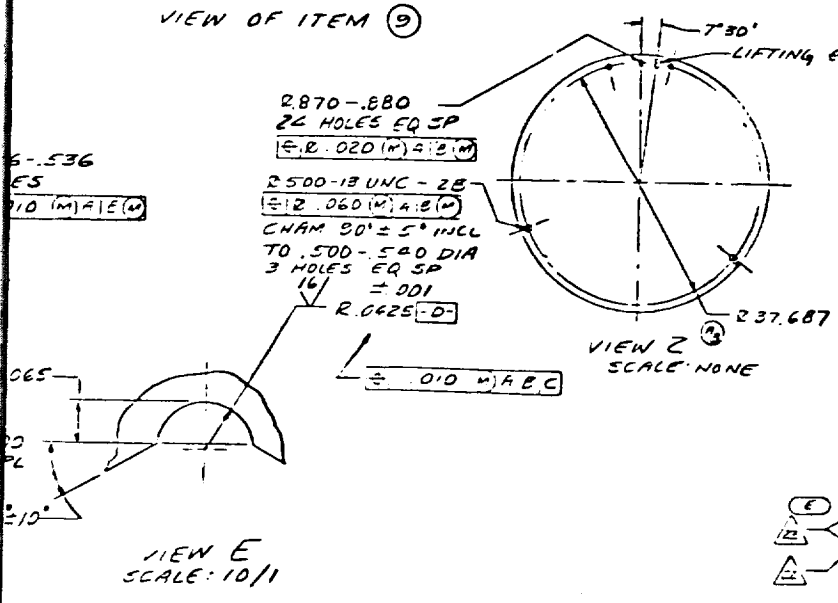
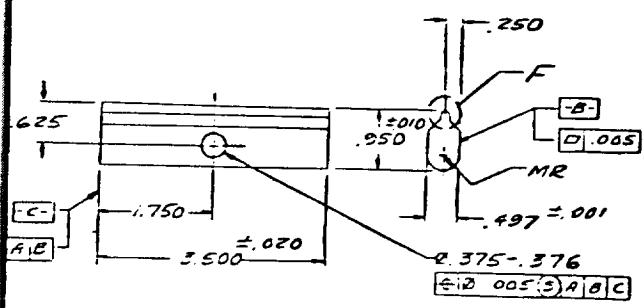
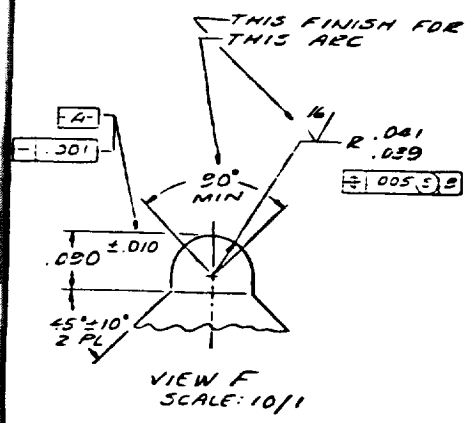
ITEM 8



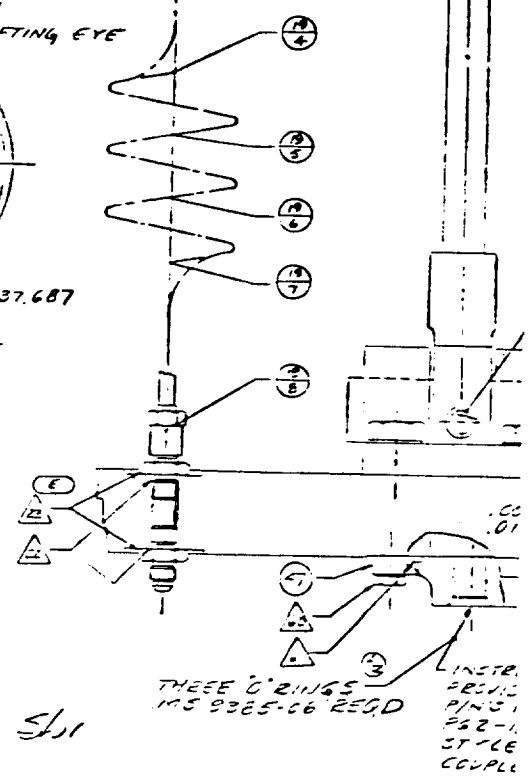
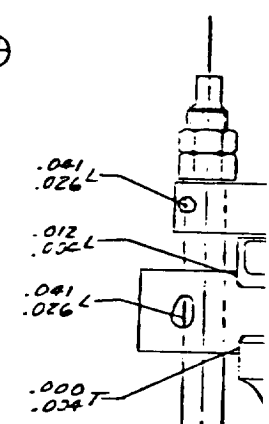
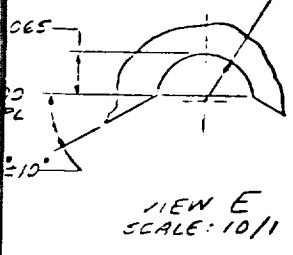


①② TUBE COORDINATES

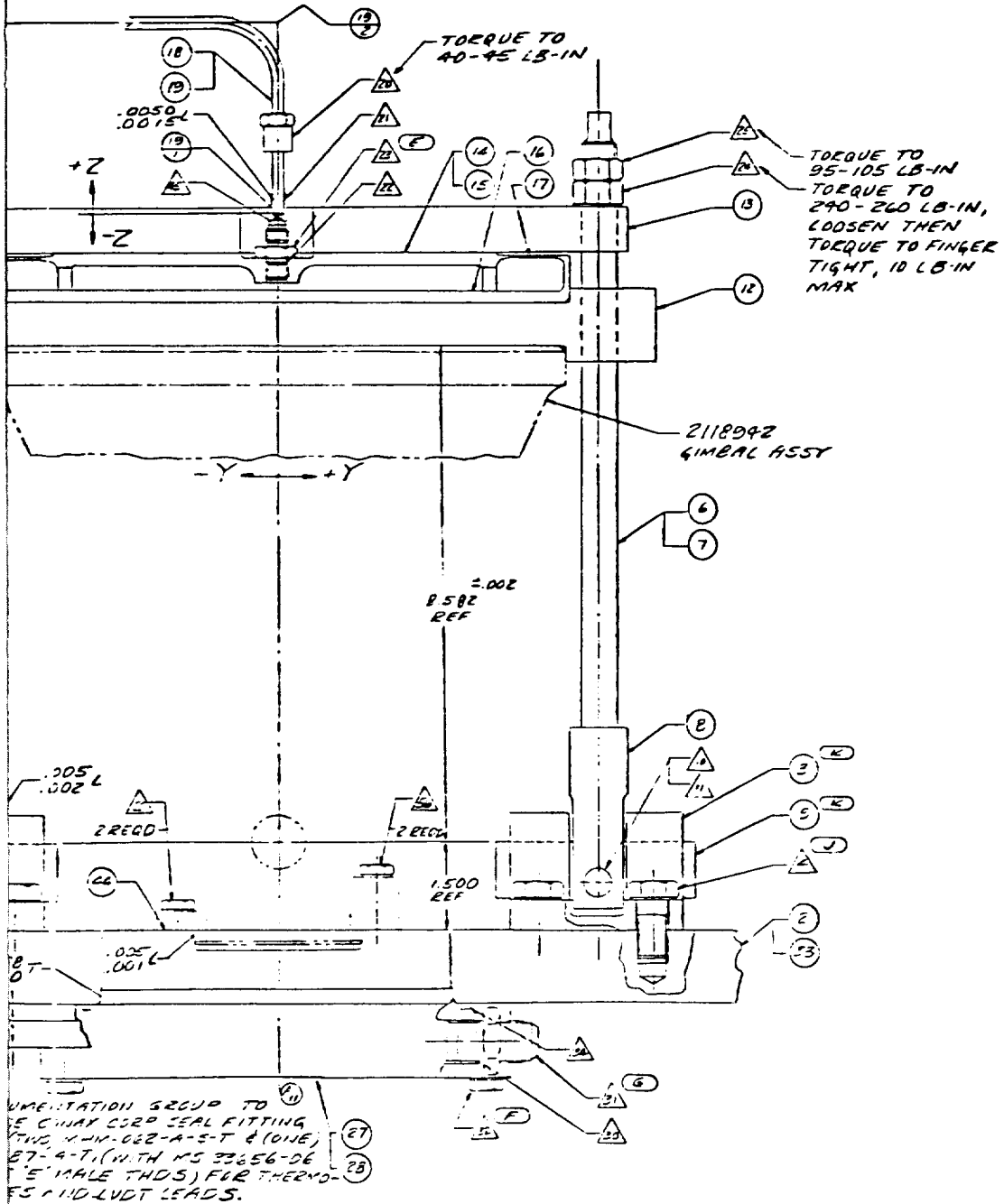
ITEM	PT	X	Y	Z	R
18	REP	.000	.000	-.165	—
19	1	.000	.000	.000	—
	2	.000	.000	3.500	1.000
	3	.000	-10.000	3.500	1.000
	4	.000	-10.000	-6.000	1.000
	5	.000	-10.000	-7.000	1.000
	6	.000	-10.000	-8.000	1.000
	7	.000	-10.000	-9.000	1.000
	8	.000	-10.000	-11.767	—
18	REP	.000	-10.000	-11.872	—



6-.536
ES
1/10 (M) A E (M)



L-240212 S/L

[illegible]

[illegible]

27. ITC
TO
KN
28. DE
CE
150
AS
DE
OF
29. LE
PE

		24	MS9576-085	O'RING	AMS 5785 SST				
	1	33		PLATE SET					NSGR
		32	MS9490-22	BOLT	AMS 5781 SST			275-24 UNF-28 LENGTH 1.155	
	2	31	MS9193-08	NIPPLE	AMS 5609 SST			750-16 UNF-28	
	2	30	MS9584	GASKET	AMS 6021 AL ALLOY			760107-01 UNF-28 LENGTH 1.155	
		29	SH 1	PLUG	AMS 6061 T6				NSGR
		28	SH 2	BLOCK	AMS 6061 T6				NSGR
		27	SH 2	BLOCK-COOL ASST OF				NOTE 14	NSGR
	1	26		LOAD CELL				NOTE 15	NSGR
	2	25	MS9361-16	NUT	AMS 5785 OR 5787			625-18 UNF-28	
	2	24	MS9356-16	NUT	AMS 5785 OR 5787			625-18 UNF-28	
	3	23	MS9193-02	NIPPLE	AMS 5609 SST				
	3	22	MS9385-02	O'RING	AMS 5787				
		21	MS9483-03	FERRULE	AMS 5046 SST				
		20	MS9197-03	NUT	AMS 5046 SST			NOTE 13	
		19		TUBE	AMS 5571 SST			NOTE 6	NSGR
	1	18		TUBE- ASST OF				NOTE 5,7	NSGR
	1	17		PLATE	AMS 547 SST				NSGR
	1	16		PLATE	AMS 547 SST				NSGR
	1	15		PLATE	AMS 547 SST				NSGR
	X	14		ACTUATOR- ASST OF					SEE NOTES
		13		PLATE	AMS 2014 T6			NOTE 14	NSGR
		12		PLATE	AMS 2014 T6			NOTE 14	NSGR
	3	11	MS924-FAS	PIN-COTTER	AMS 7211 SST				
	3	10	MS9847-25	PIN	AMS 5785 SST			62-2744-5-48	
	2	9		BLADE	AMS 5465 CO ALLOY			NOTE 22	NSGR
	1	8		LOG	AMS 5465 NI ALLOY				NSGR
	1	7		ROD	AMS 5465 NI ALLOY				NSGR
	X	2	6	ROD-ASST OF				NOTE SPEC PARA 1-55	NSGR
		1	5	SH 3	AMS 5465 T6			NOTE 14	NSGR
		28	4	MS9494-07	BOLT	AMS 5781 SST		500-28 UNF-28 LENGTH 1.000	
	2	3		CLEVIS	AMS 5785 CO ALLOY			NOTE 22	NSGR
		2		PLATE	AMS 547 SST			NOTE 14	NSGR
	X	1		RIG ASST					NSGR

LAYOUT FOLLOW-UP LIST

MS 5 55, 60, 68, 69, 70 & 71 ARE
BE USED TO DETERMINE THE RIGS
LIFE EDGE FRICTION
TERMINE THE DEFLECTION AT THE
ENTER OF ITEM 27 UNDER THE
100 LB LOAD. ADD SHIMS, ITEM 44
NEED TO COMPENSATE FOR THIS
DEFLECTION DURING THE OPERATION
THE TEST.
AK TEST PER PTM, NO LEAKAGE
RMITTED

-240212

SHEET 1/A

SOURCE APPROVAL, REQUIREMENTS

5. A CONTINUOUS (SEE ARI 10) RECORDING OF THE TEST

THE RECORDING SHOULD BE MADE AT THE FOLLOWING INTERVALS:

1. THE RECORDING SHOULD BE MADE AT THE FOLLOWING INTERVALS:

2. THE RECORDING SHOULD BE MADE AT THE FOLLOWING INTERVALS:

3. THE RECORDING SHOULD BE MADE AT THE FOLLOWING INTERVALS:

4. THE RECORDING SHOULD BE MADE AT THE FOLLOWING INTERVALS:

5. THE RECORDING SHOULD BE MADE AT THE FOLLOWING INTERVALS:

6. THE RECORDING SHOULD BE MADE AT THE FOLLOWING INTERVALS:

7. THE RECORDING SHOULD BE MADE AT THE FOLLOWING INTERVALS:

8. THE RECORDING SHOULD BE MADE AT THE FOLLOWING INTERVALS:

9. THE RECORDING SHOULD BE MADE AT THE FOLLOWING INTERVALS:

10. THE RECORDING SHOULD BE MADE AT THE FOLLOWING INTERVALS:

THIS DOCUMENT IS THE PROPERTY OF THE PRATT & WHITNEY CORPORATION AND IS LOANED TO THE RESEARCHER ON THE CONDITION THAT IT IS NOT TO BE REPRODUCED, COPIED, OR IN ANY MANNER, OR USED FOR ANY PURPOSE, WITHOUT THE WRITTEN PERMISSION OF THE PRATT & WHITNEY CORPORATION. IT IS TO BE RETURNED TO THE PRATT & WHITNEY CORPORATION AT THE END OF THE TEST. IT IS TO BE KEPT IN A SAFE PLACE AND NOT TO BE USED FOR ANY OTHER PURPOSE. IT IS TO BE KEPT IN A SAFE PLACE AND NOT TO BE USED FOR ANY OTHER PURPOSE. IT IS TO BE KEPT IN A SAFE PLACE AND NOT TO BE USED FOR ANY OTHER PURPOSE.

PRATT & WHITNEY CORPORATION

RESEARCHER'S SIGNATURE

DATE

TEST NUMBER

TEST DATE

TEST TIME

TEST LOCATION

TEST RESULTS

TEST COMMENTS

TEST SIGNATURE

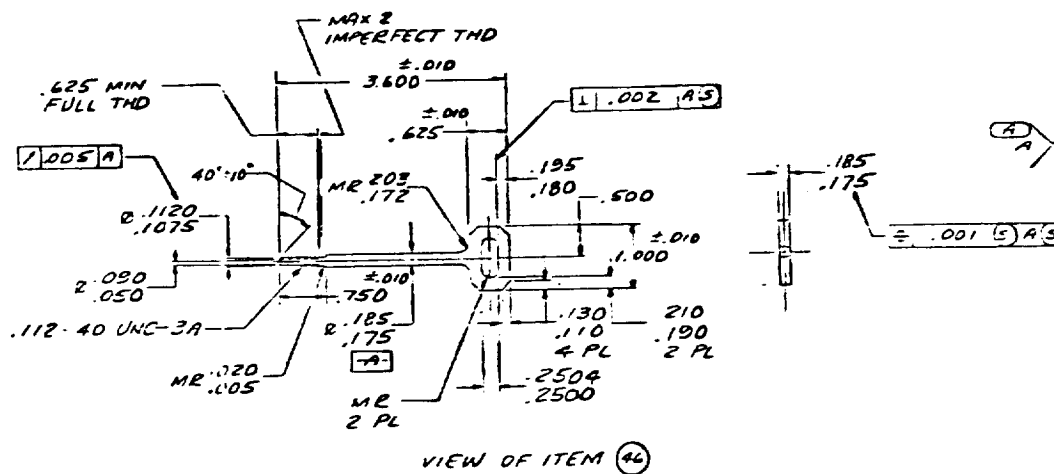
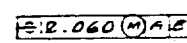
TEST DATE

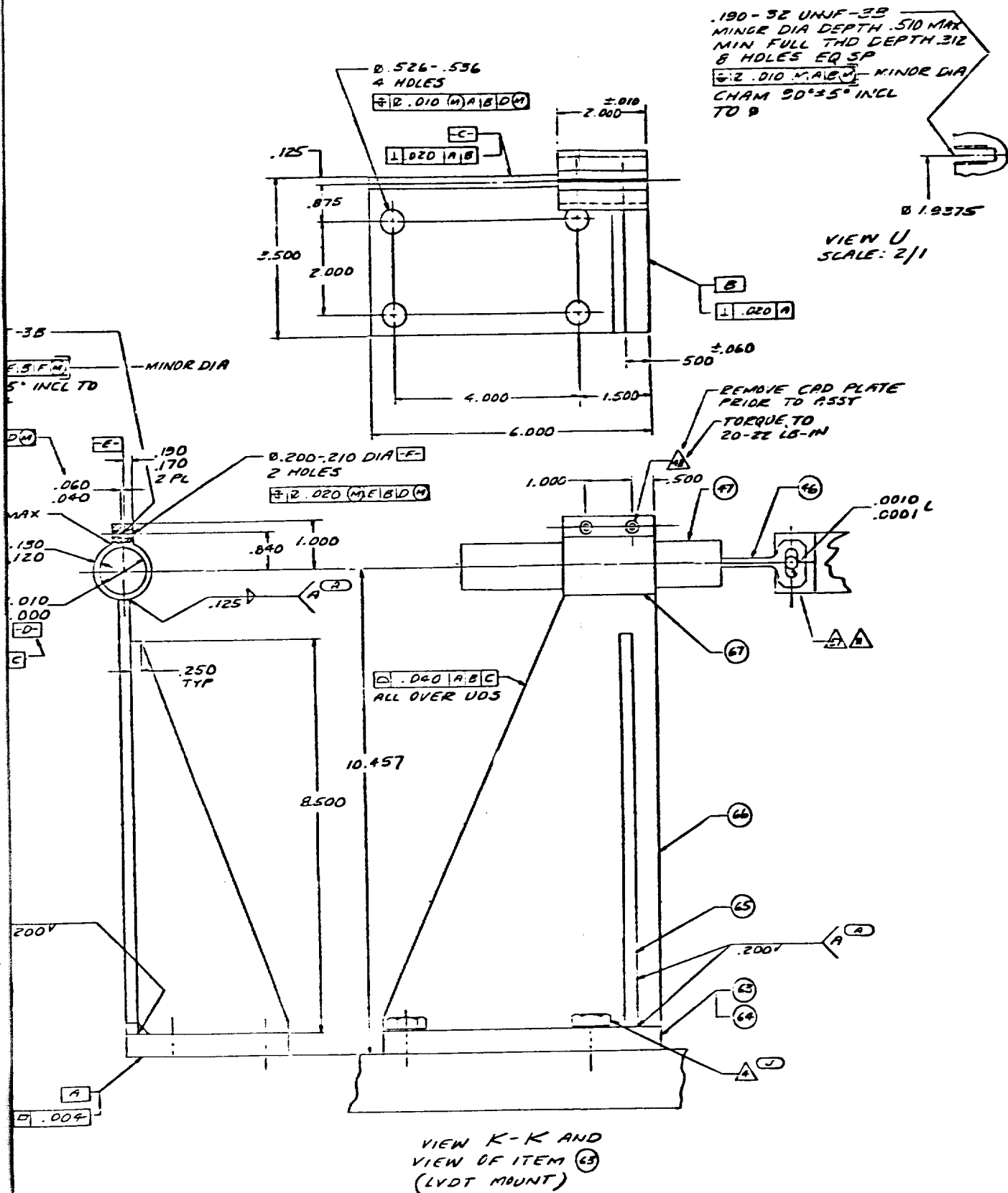
TEST TIME

TEST LOCATION

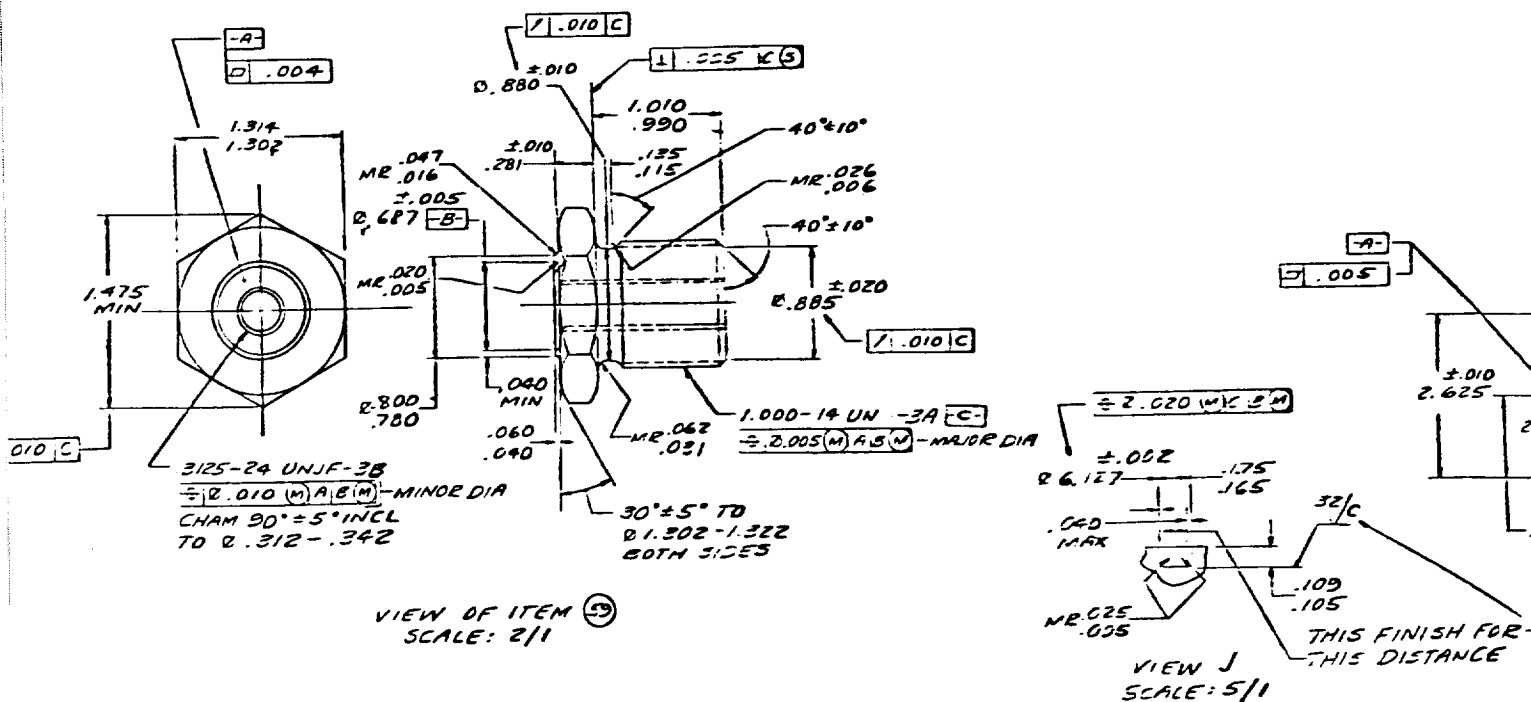
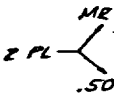
TEST RESULTS

TEST COMMENTS

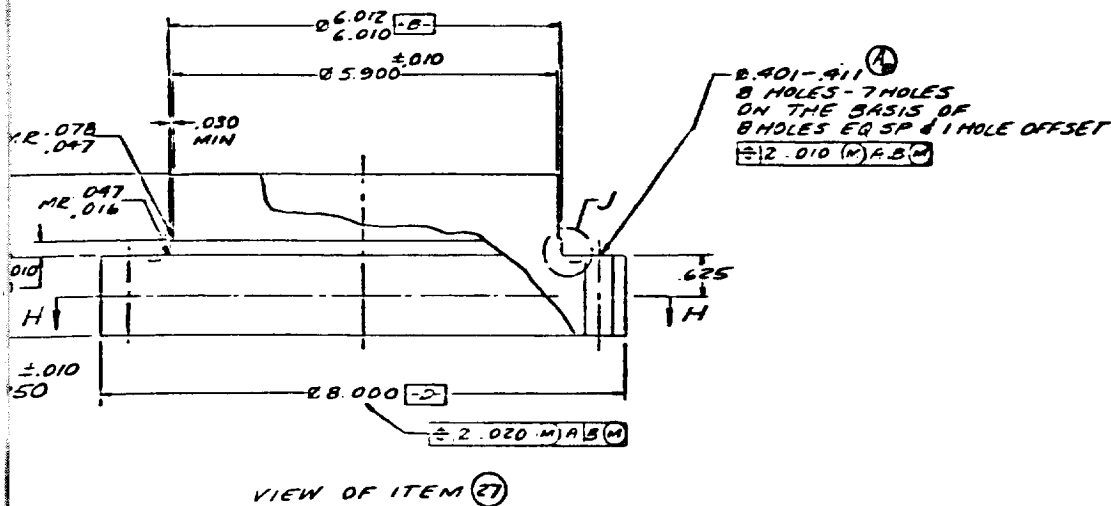
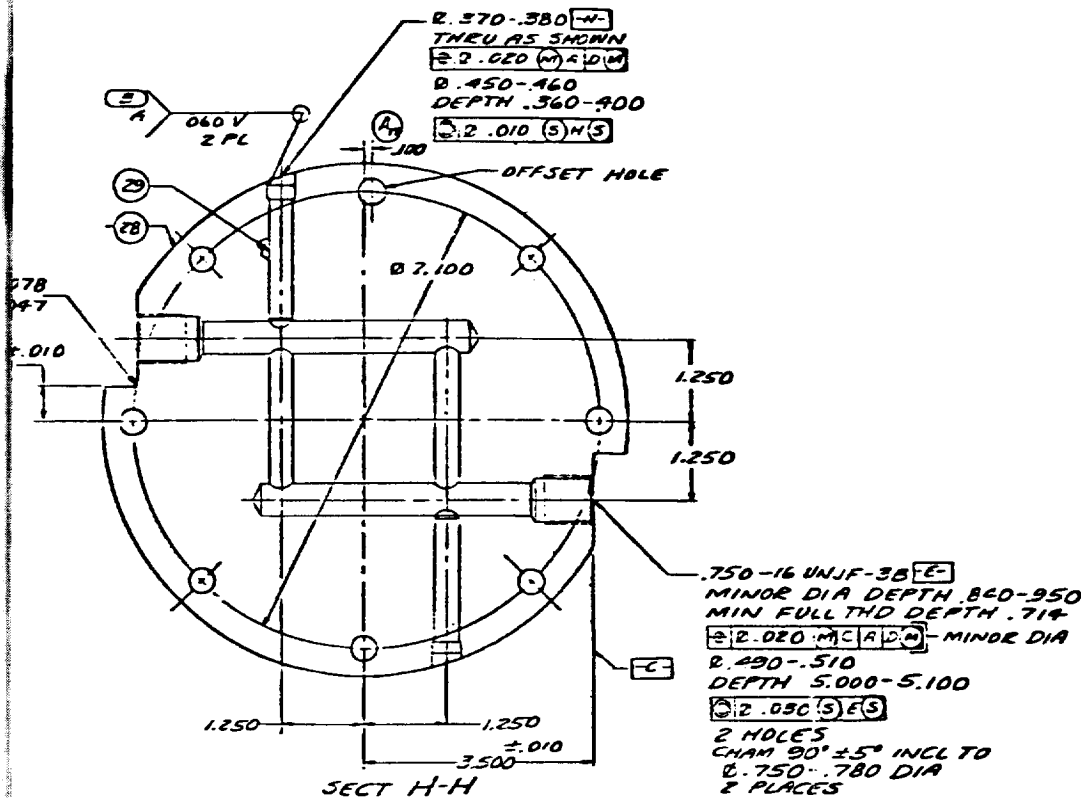
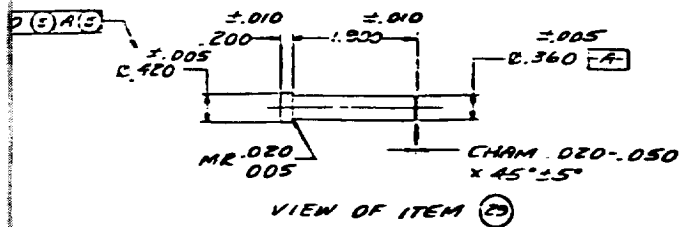




L-240212 SL2



ALTERATION	DATE	REVISION
(13) WAS PIPE TWO A (16) ADDED VIEW FOR AND RELATED INFO	11/11/51	85-711-AD6885
(17) ADD DIMENSION (18) ADD OFFSET FOR	11/11/51	85-711-AD6885

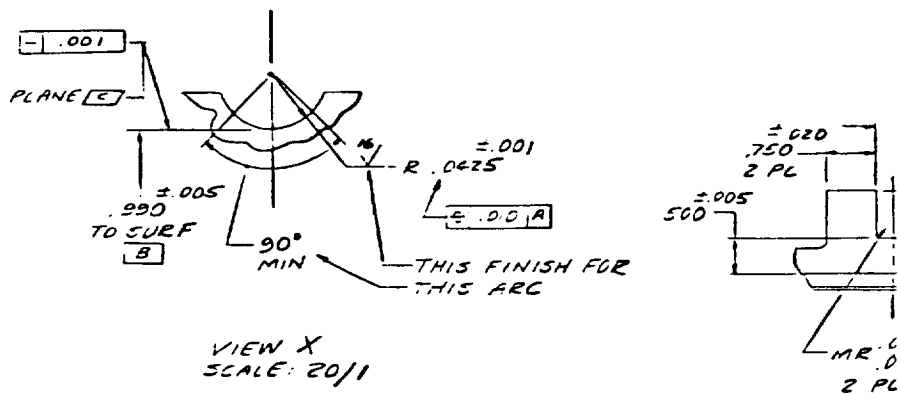
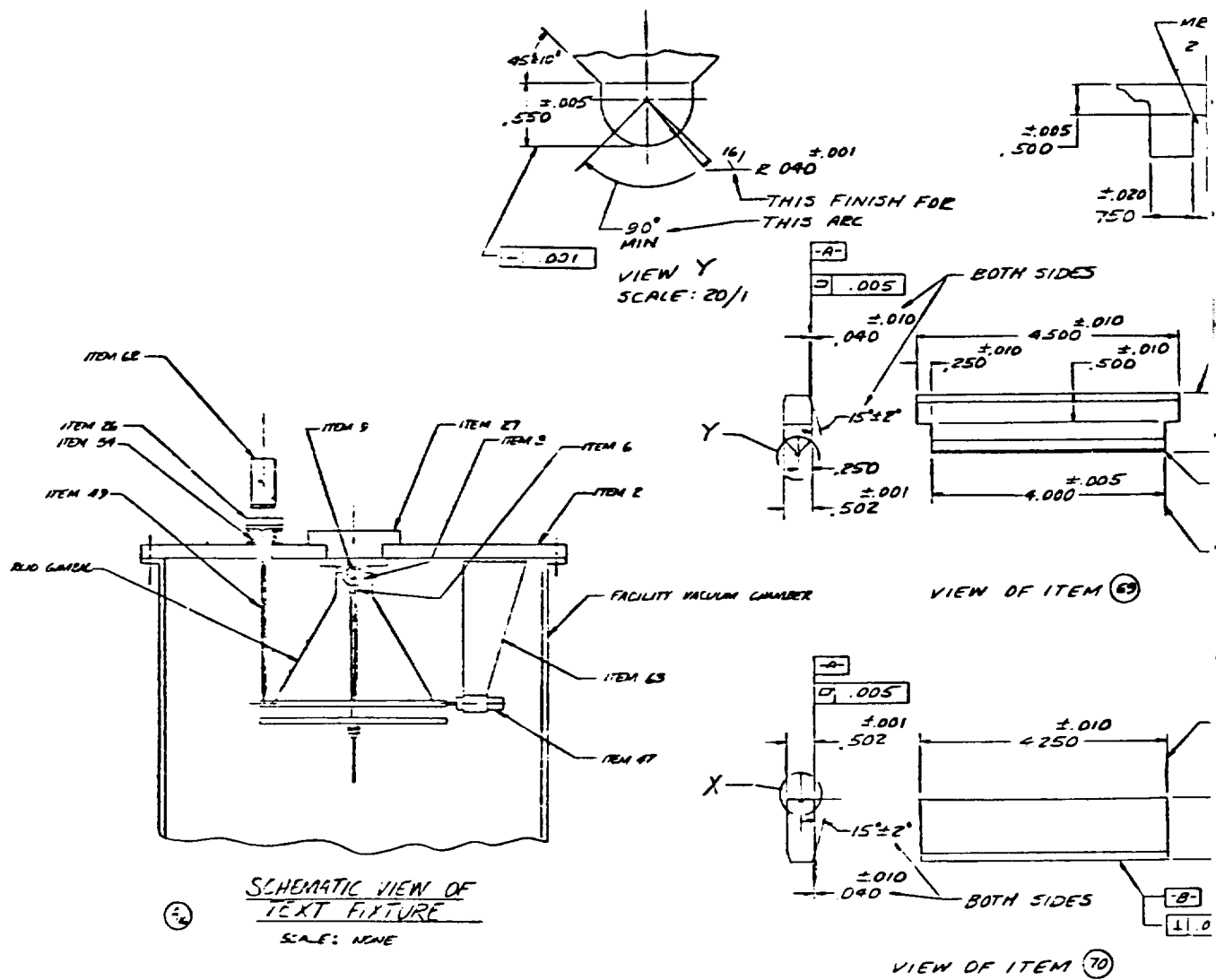


L-240212
SHEET 2A

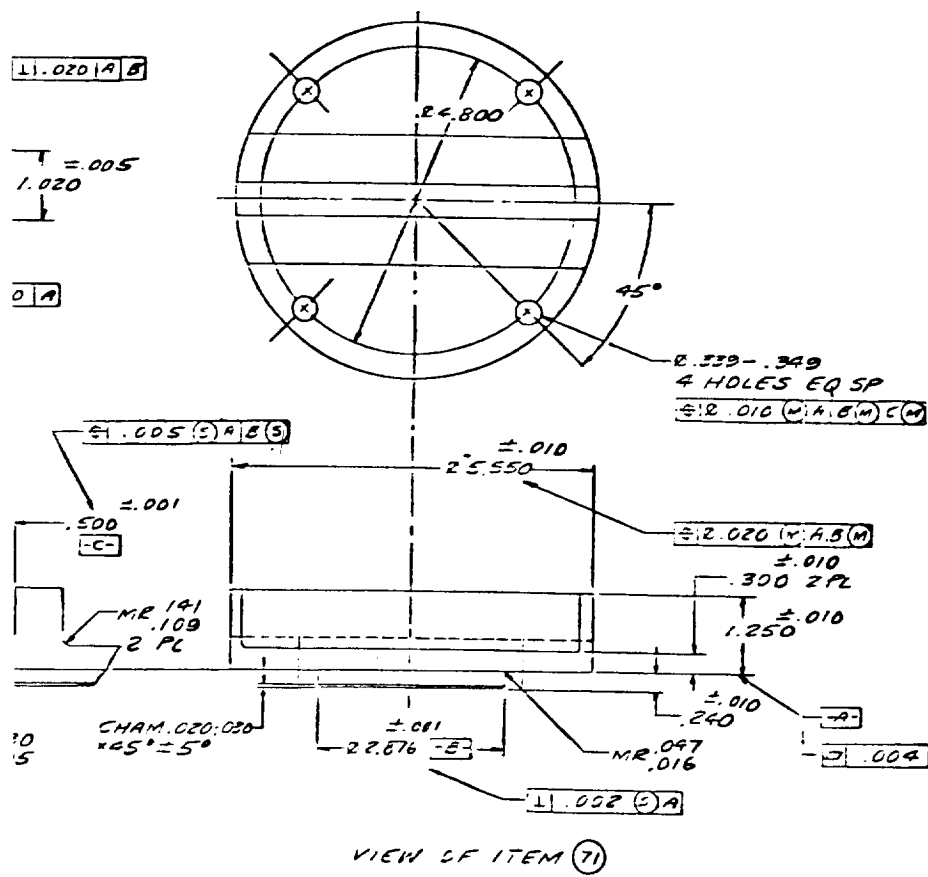
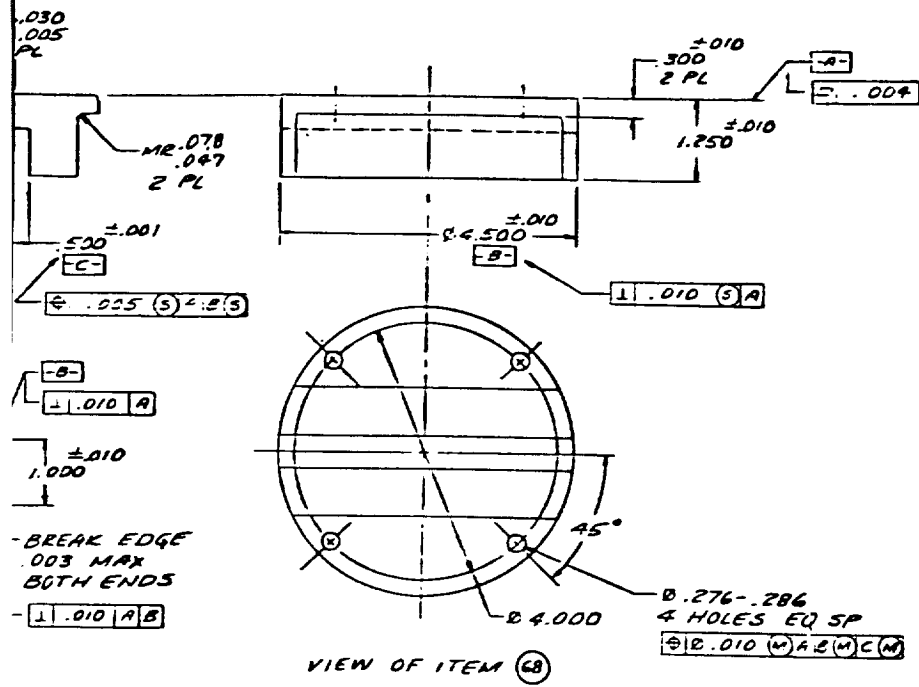
PRATT & WHITNEY AIRCRAFT
CONTROLLED
Revised
2/27/52
L-R-PS

PRELIMINARY	77645
DESIGNED BY	DATE
CHECKED BY	DATE
APPROVED BY	DATE
REVISIONS	
1. 2.15	
2. 2.15	
3. 2.15	
4. 2.15	
5. 2.15	
6. 2.15	
7. 2.15	
8. 2.15	
9. 2.15	
10. 2.15	
11. 2.15	
12. 2.15	
13. 2.15	
14. 2.15	
15. 2.15	
16. 2.15	
17. 2.15	
18. 2.15	
19. 2.15	
20. 2.15	
21. 2.15	
22. 2.15	
23. 2.15	
24. 2.15	
25. 2.15	
26. 2.15	
27. 2.15	
28. 2.15	
29. 2.15	
30. 2.15	
31. 2.15	
32. 2.15	
33. 2.15	
34. 2.15	
35. 2.15	
36. 2.15	
37. 2.15	
38. 2.15	
39. 2.15	
40. 2.15	
41. 2.15	
42. 2.15	
43. 2.15	
44. 2.15	
45. 2.15	
46. 2.15	
47. 2.15	
48. 2.15	
49. 2.15	
50. 2.15	
51. 2.15	
52. 2.15	
53. 2.15	
54. 2.15	
55. 2.15	
56. 2.15	
57. 2.15	
58. 2.15	
59. 2.15	
60. 2.15	
61. 2.15	
62. 2.15	
63. 2.15	
64. 2.15	
65. 2.15	
66. 2.15	
67. 2.15	
68. 2.15	
69. 2.15	
70. 2.15	
71. 2.15	
72. 2.15	
73. 2.15	
74. 2.15	
75. 2.15	
76. 2.15	
77. 2.15	
78. 2.15	
79. 2.15	
80. 2.15	
81. 2.15	
82. 2.15	
83. 2.15	
84. 2.15	
85. 2.15	
86. 2.15	
87. 2.15	
88. 2.15	
89. 2.15	
90. 2.15	
91. 2.15	
92. 2.15	
93. 2.15	
94. 2.15	
95. 2.15	
96. 2.15	
97. 2.15	
98. 2.15	
99. 2.15	
100. 2.15	

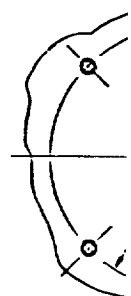
THIS DRAWING IS THE PROPERTY OF PRATT & WHITNEY AIRCRAFT COMPANY AND IS LOANED TO THE USER UNDER THE CONDITION THAT IT IS NOT TO BE REPRODUCED, COPIED, OR IN ANY MANNER, OR USED FOR ANY PURPOSE OTHER THAN THAT FOR WHICH IT WAS LOANED. IT IS TO BE RETURNED TO PRATT & WHITNEY AIRCRAFT COMPANY AT THE END OF THE LOAN PERIOD. IT IS TO BE KEPT IN A SAFE PLACE AND NOT TO BE LOANED TO ANY OTHER PERSON OR ORGANIZATION. IT IS TO BE KEPT IN A SAFE PLACE AND NOT TO BE LOANED TO ANY OTHER PERSON OR ORGANIZATION. IT IS TO BE KEPT IN A SAFE PLACE AND NOT TO BE LOANED TO ANY OTHER PERSON OR ORGANIZATION.



L-240212 SL3



.005
.001



THE UNIVERSITY OF MICHIGAN LIBRARY
400 TAPSCOTT DRIVE
ANN ARBOR, MICHIGAN 48106-1000
TEL: (313) 763-7000
FAX: (313) 763-7000
WWW: WWW.LIBRARY.MICHIGAN.EDU

SALT MARSHES

FELICIA

SECRETARY UNIT

GUNZ-7000

TEST FIRE

APPENDIX E
CENTAUR ENGINE GIMBAL FRICTION CHARACTERISTICS UNDER SIMULATED
THRUST LOAD

NASA Technical Memorandum 87335

Centaur Engine Gimbal Friction Characteristics Under Simulated Thrust Load

James W. Askew
Lewis Research Center
Cleveland, Ohio

September 1986



Trade names or manufacturers' names are used in this report for identification only. This usage does not constitute an official endorsement, either expressed or implied, by the National Aeronautics and Space Administration.

CENTAUR ENGINE GIMBAL FRICTION CHARACTERISTICS UNDER SIMULATED THRUST LOAD

James W. Askew
National Aeronautics and Space Administration
Lewis Research Center
Cleveland, Ohio 44135

ABSTRACT

An investigation was performed at NASA Lewis Research Center to determine the friction characteristics of the engine gimbal system of the Centaur upper stage rocket. Because the Centaur requires low-gain autopilots in order to meet all stability requirements for some configurations, control performance (response to transients and limit-cycle amplitudes) depends highly on these friction characteristics. Forces required to rotate the Centaur engine gimbal system were measured under a simulated thrust load of 66 723 N (15 000 lb) and in an altitude/thermal environment. A series of tests was performed at three test conditions: ambient temperature and pressure, ambient temperature and vacuum, and cryogenic temperature and vacuum. Gimbal rotation was controlled, and tests were performed in which rotation amplitude and frequency were varied by using triangular and sinusoidal waveforms. Test data revealed an elastic characteristic of the gimbal, independent of the input signal, which was evident prior to true gimbal sliding. The torque required to initiate gimbal sliding was found to decrease when both pressure and temperature decreased. Results from the low amplitude and low frequency data are currently being used in mathematically modeling the gimbal friction characteristics for Centaur autopilot performance studies.

NOMENCLATURE

CF coulomb friction
K slope of spring constant of gimbal

- K1 slope of spring constant of test rig
- T friction torque
- δ rotation angle
- $\dot{\delta}$ angular velocity

INTRODUCTION

Thrust vectoring, one method used for space vehicle flight control, is typically accomplished by a servocontrolled actuator system, which rotates a rocket engine nozzle about a single gimbal point. Such a system is incorporated in the Centaur upper stage vehicle. The dynamics of rotating the engine about the gimbal point depends highly on the friction characteristics of the gimbal. For Centaur, a hydraulic power unit is used to actuate engine motion about a two-axis gimbal system that mounts the engine to the vehicle. The gimbal system also provides the load path into the vehicle structure for engine thrust.

Background

The design of the Centaur D1-A powered phase autopilot and the resulting assessment of control performance depended on reliable, test-verified mathematical models. These mathematical models, over the history of the Centaur D1 and Centaur D1-A, have been shown to be accurate representation of the hardware and software flown. This has been demonstrated through component level testing and flight performance evaluation. The current design of the autopilot was first flown on April 5, 1973. Payloads have ranged in weight from approximately 500 to 3085 kg (1100 to 6800 lb). The autopilot configuration has remained constant with variations only in constants required for optimization. This design is also being applied to the shuttle/Centaur for those payloads which have dynamic and weight characteristics similar to payloads previously flown on D1-A. Classes of payload which are different than those previously flown may require a redesign of the autopilot control

law. In particular, for payloads which require low-gain autopilots, performance depends highly on the friction characteristics of the engine gimbal. This high dependence on engine gimbal friction resulted in a test program to further refine a friction mathematical model.

In the time period between 1962 and 1965, two tests were run to determine the friction characteristics of the engine gimbal. A hot firing test was run at NASA Lewis Research Center, and a static load test was run at Pratt & Whitney, the engine manufacturer. Both of these tests showed values of coulomb friction from 71 to 91 J (52 to 67 ft-lb) per plane. These results were well below the specified requirement of 271 J (200 ft-lb) set by General Dynamics Space System Division for a 66 723-N (15 000-lb) thrust engine.

Purpose

A more accurate measurement of the friction characteristics of the present Centaur gimbal system was needed to properly assess autopilot performance for certain shuttle/Centaur applications. The purpose of this test was to determine the friction characteristics of the Centaur engine (model RL10A-3-3A) gimbal system, under thrust load and in an altitude/thermal environment.

APPARATUS

Engine Mount Gimbal Assembly

The gimbal mount assemblies used for the tests were Pratt & Whitney RL10A-3-3A engine flight gimbals. The gimbal mount assembly provided a universal bearing system to allow gimbaling of the engine for thrust vectoring (Fig. 1). The gimbal assembly, as described in Ref. 1, consisted of a conical engine mount, a pedestal, and a spider block. Gimbaling was accomplished by rotation about the spider block, which connected the pedestal to the conical mount. The gimbal incorporated dry-lubricated journal bearings, which permitted gimbal movement of $\pm 4^\circ$ in a square pattern during engine operation. The gimbal assembly was secured to the test rig by four bolts, which passed

through the top of the pedestal. The gimbal assembly was instrumented with two thermocouples to monitor temperature on the pedestal and conical section during cryogenic testing.

Test Facility

The vacuum facility used in testing was the Super Bell Jar facility located at Lewis. This facility consists of two separate stainless steel bell jars; however, only one was used for the testing described. Each bell jar has a 86.36-cm (34.0-in.) diameter and is 170.18 cm (67.0 in.) high. A single 88.9-cm-diameter (35-in.-diam) oil diffusion pump was mounted on the bottom of the bell jar. Pressure in the bell jar during testing was maintained between 0.041 and 5.068 N/m² (5.88×10^{-6} and 7.35×10^{-4} psi). The gimbal mount assembly was mounted from a specially designed top flange plate (test rig, Fig. 2) with the conical section pointing downward along the bell jar axis.

A variable-displacement hydraulic pump was used during testing to provide the proper flow rate of 1.58×10^{-4} m³/sec (2.5 gal/min) and pressure of 3.45×10^6 N/m² (500 psig) needed to supply the closed-loop servocontrolled actuator. The pump was in operation only when an oscillation signal was commanded to the closed-loop servocontroller, resulting in actuator movement.

Liquid nitrogen was used in the test rig as a coolant to simulate the cryogenic temperature of the liquid oxygen tank (94 K or 170 °R). The liquid nitrogen was transferred from a conventional pressurized (1.72×10^5 N/m² or 25 psig) Dewar to the test rig cold plate by foam-insulated lines. However, before the test rig was submitted to cryogenic temperature, a gaseous nitrogen purge on the bell jar was performed. This evacuated moisture from the environment to prevent ice from forming on the gimbal (test rig). Gaseous nitrogen was also used to pressurize the pneumatic load applicator (bellows), which was used to apply a compression load to the gimbal for simulating engine thrust.

Test Rig

The test rig used to determine the gimbal friction characteristics was designed to incorporate a simulated thrust load of 66 723 N (15 000 lb), a space environment, and cryogenic temperatures. The fixture was optimized around two minimum-friction knife edge load rods (see Fig. 3). Further consideration included a common axis of rotation for the load rods and the journal bearings, constant load application throughout gimbal position, and a closed-loop response system.

The rig was designed and assembled by Pratt & Whitney. The basic design consisted of a large steel plate which was placed on one end of the environmental vacuum chamber (see Fig. 2). Mounted on the plate was an aluminum plug with passages for flowing liquid nitrogen. Inside the vacuum chamber was the gimbal mount assembly, the calibrated knife edge load rods, and the pneumatic bellows plate for applying load. Through the steel base plate, which was sealed with a bellows, the actuator rod hydraulically actuated the gimbal. Gaseous nitrogen, used to apply load to the bellows plate, passed through a bulkhead fitting to the inside of the vacuum chamber. The other testing fluids, liquid nitrogen for cooling and hydraulic oil for actuation, were kept external to the chamber.

PROCEDURE

Gimbal Movements

Gimbal position was controlled by a servocontrolled actuator. The input signals for triangular and sinusoidal wave patterns were supplied by a wide-range-frequency function generator. These input command signals were sent to the servoamplifier, which operated the actuator piston and rod. A linear variable differential transformer (LVDT) position feedback transducer was mounted normal to the piston rod (see Fig. 3). The LVDT measured the displacement of the actuator piston, which is relative to the gimbal

displacement. The signals from the LVDT were then fed back to the servoamplifier. The signals from the servoamplifier were recorded on a digital data recorder capable of recording 500 samples/sec and on a direct-writing oscillograph.

The LVDT feedback transducer calibration, which determined the output of the feedback transducer in volts per degree of gimbal displacement, was made prior to testing. The procedures (gimbal movement patterns) used for the various tests are described in the section Test Conditions.

Force Measurements

At the beginning of each test sequence, the gimbal was loaded with a compression force of 66 723 N (15 000 lb), representing the thrust load on the gimbal in flight. This was accomplished by pressurizing the bellows placed between plates A and B, shown in Fig. 3. The force generated between the two plates placed the gimbal and the two tension rods mounted on knife edges in compression. The knife edges were aligned to coincide with the centerline of the axis of rotation. This minimized forces (torques) from the loading mechanism as the gimbal rotated.

Forces applied to the gimbal were determined by a universal flat compression-tension load cell, which measured the forces being applied to the actuator (Fig. 3). The load cell was mounted on a support coaxially with the actuator rod, below the actuator. The location of the load cell was essential to the applied forces in order to neglect inertial forces. Loads to the load cell were applied through the actuator rod, which was concentric with the threaded hole at the center of the cell. Loads measured away from the support mount were considered tension loads, with positive signals. Loads measured toward the support mount were considered compression loads, with negative signals. The load cell signals were also recorded on the digital data recorder and the oscillograph.

The load cell calibrations, which determined the output signal in volts per newton (pound of force), were also made prior to testing. The applied forces were converted to applied torques by multiplying the force by the distance from the actuator rod to the pivot point of the gimbal.

Test Conditions

Three different test conditions were used during testing: (1) ambient temperature and pressure, (2) ambient temperature and vacuum, and (3) cryogenic temperature and vacuum. Test conditions 1 and 2 consisted of four test sequences each. The sequences were performed at frequencies of 0.1, 0.5, 1.0, and 2.0 Hz at an amplitude of 0.25° relative to the null position. Each sequence had a triangular wave input signal. Test condition 3 consisted of 12 sequences, which comprised both triangular and sinusoidal wave input signals. At this test condition, test sequences were performed at frequencies of 0.1, 0.5, 1.0, and 2.0 Hz, with amplitudes of 0.25° and 2.0° relative to the null position. See Tables I and II for test results of each sequence.

After completion of test condition 1, the bell jar was pumped down to a vacuum environment of 0.041 N/m^2 (5.88×10^{-6} psi), or below. Prior to test condition 3, the cold plate was cooled to a temperature of 94 K (170 °R).

THEORETICAL INVESTIGATION

Solid Friction

Solid friction is a quasi-static phenomenon that occurs when two solid surfaces are subjected to contact bond stress by external or inertial forces.² Both coulomb friction (CF) and static friction (stiction) are involved. The coulomb friction is related to the interface bond rupture stress, whereas the static friction, or stiction, is related to the maximum, or ultimate, stress of the interface bond. Figure 4 depicts the general characteristics of solid friction. When the velocity is equal to zero, stiction occurs. Further, as

velocity is applied, the friction force (torque) drops to a lower level, coulomb friction. This friction remains constant as the velocity increases.

Solid friction encompasses two different types of friction: sliding friction and rolling friction. However, since the gimbal assembly incorporates a journal bearing, rolling friction will be our primary concern.

Rolling Friction

Early theories of rolling friction attributed it to interfacial slip between the rolling element and the surface. However, rolling friction is now attributed to the deformation losses in the solid itself, although some slip may occur. With elastic solids, where no permanent deformation occurs, rolling friction is attributed to hysteresis losses in the solid. In rolling friction, the interface cohesively bonded regions are compression stressed on the front side of the contact area and tension stressed on the back. The process of rolling friction starts from an unstressed region between two solid surfaces. Thus, as the strain or relative displacement of the surfaces increases, the surfaces are elastically stressed until a critical stress between the two surfaces is reached. This critical stress is the interface bond rupture stress (coulomb friction). After the interface bond has been ruptured, the rolling surface begins to slide, and the rolling friction becomes sliding friction. The coulomb friction value remains constant until the relative displacement is reversed. The same effect occurs in the reverse direction, forming an elastic hysteresis. This force-versus-motion characteristic is similar to that shown in Fig. 5. Additional information can be obtained from Refs. 3 to 5.

RESULTS AND DISCUSSION

A series of tests was performed on five flight gimbals; however, only data for gimbals designated 759 and 94 are presented in Tables I and II. Graphic representations of the experimental data are depicted in Figs. 6 to 8. Figure 6 shows the contrasting characteristics of the high and low amplitudes,

whereas Fig. 7 depicts the contrast in test conditions. The data graphed in Figs. 6 and 7 have frequencies of 2 and 1 Hz, respectively. Figure 8 compares the characteristics of the input signals, sinusoidal and triangular, at an amplitude of 0.25° and a frequency of 0.1 Hz. Both pitch and yaw axes of rotation, on each gimbal, were tested under the three conditions specified earlier. An initial test sequence was run at the beginning of testing on each gimbal to determine the break-in characteristic. The force (torque) levels required to move the gimbals decreased with increasing number of cycles, leveling off after about 10 cycles. This data is not presented here.

Before each series of tests, several calibrations of the test rig were performed with a dummy gimbal to determine the inherent frictional characteristic of the test rig. This device had dimensions similar to a flight gimbal assembly, except that a knife edge replaced the pedestal and spider block. The data from these calibrations are not presented here. However, the data showed the test rig to have a linear variation (K_1) of increasing force (torque) with increasing relative gimbal displacement (see Fig. 5(a)). This variation K_1 was subtracted from data taken during gimbal testing. This data reduction resulted in a gimbal friction characteristic similar to that shown in Fig. 5(b).

Early testing on the RL-10 engine gimbal mounts,⁶ showed the gimbal friction characteristic as shown in Fig. 4, for solid friction. However, in this test, data showed the friction characteristic to be as that of rolling friction (see Fig. 5(b)).

The low-amplitude triangular and sinusoidal wave oscillations gave values of coulomb friction in a range of 90 to 129 J (66 to 95 ft-lb) in the pitch axis of rotation, and a range of 61 to 207 J (45 to 153 ft-lb) in the yaw axis. A linear variation of increasing force (torque) with increasing gimbal rotation

occurred when motion was reversed. This slope (K) lasted over an interval of 0.2° and decreased with increasing frequency (see Figs. 5(a), 6, and 8).

The high-amplitude triangular wave resulted in lower values of coulomb friction, ranging from 34 to 125 J (25 to 92 ft-lb) in the pitch axis and from 12 to 201 J (9 to 148 ft-lb) in the yaw axis. A piecewise linear variation of increasing force (torque) with increasing rotation was observed. This was displayed as a steep slope (K) when motion was reversed, lasting an interval of 0.2° , and a shallow slope (K_1) as motion continued. The steep slope K is similar to the slope observed in the low amplitude tests, and it is attributed to the elastic stressing of the interface bond between the rolling and stationary surfaces of the gimbal journal bearing. This type of characteristic is actually that of a simple rotational spring, with sliding after reaching the coulomb friction. The shallow slope K_1 is attributed to the linear variation found in the test rig (see Figs. 5(a), 6, and 7).

Environmental conditions were observed to affect the coulomb friction values. Test condition 1 results showed higher values of coulomb friction than test conditions 2 and 3. Furthermore, test condition 2 gave values of coulomb friction greater than test condition 3. From this, it was evident that coulomb friction decreased with decreasing pressure and/or temperature. The decline in coulomb friction leveled off after the pressure and/or temperature were stabilized, at the respective test conditions.

Another phenomenon that was apparent during testing was that, as the frequency increased, the width of the hysteresis loop decreased. This can be seen by comparing the high amplitude curve (frequency of 2.0 Hz) of Fig. 6 with the curves in Fig. 7 (frequency of 1.0 Hz).

It should be noted that the large values of coulomb friction presented in Table II for gimbal 759 yaw axis reflect a suspected deficiency in the quality

of the journal bearing in that particular axis. This was not observed in any other gimbal tested, and was isolated to gimbal 759 yaw axis.

CONCLUDING REMARKS

An investigation was conducted to determine the coulomb friction characteristics of the Centaur launch vehicle gimbal system. Data have been presented for a number of conditions for both pitch and yaw axes. The experimental data showed that torques required to rotate the gimbal had elastic characteristics, where the torques were proportional to the rotational displacement up to a certain value beyond which the gimbal would rotate with small increases in torque. Coulomb friction is defined as the maximum applied torque (breakaway torque) that occurs prior to gimbal sliding. The gimbal friction characteristic is similar to that of rolling friction. Furthermore, environmental effects were shown to have a major influence on the coulomb friction, which decreased with both pressure and temperature. It has also been shown that the elastic characteristics of the gimbal are independent of the input signal.

After a review of the experimental data, it was decided to use the low amplitude and low frequency data for mathematically modeling the gimbal friction characteristics for Centaur autopilot performance studies.

The results of this test are based on the Centaur gimbal system. However, the characteristics may be applied to any launch vehicle gimbal system that incorporates journal bearings.

Further tests will be performed on the Centaur tank structure, where the gimbal is attached, to determine the contribution of tank stiffness to the elasticity of the system.

REFERENCES

¹RL10 Liquid Rocket Engine, Service Manual, Model RL10-3-3A, Pratt and Whitney Aircraft, Feb. 15, 1982.

²Dohl, P.R., "A Solid Friction Model," TOR-0158(3107-18)-1, Aerospace Corporation, May 1968.

³Bowden, F.P. and Tabor, D., The Friction and Lubrication of Solids, Part II, Clarendon Press, London, 1964.

⁴Rabinowicz, E., Friction and Wear of Materials, Wiley, 1965.

⁵Bisson, E.E. and Anderson, W.J., "Advanced Bearing Technology," NASA SP-38, 1964.

⁶Antl, R.J., Vincent D.W., and Plews, L.D., "Static and Dynamic Characteristic of Centaur Gimbal System Under Thrust Load," NASA TM X-1205, 1966.

TABLE I. - SUMMARY OF EXPERIMENTAL DATA IN PITCH AXIS

Gimbal number	Waveform	Frequency, Hz	Amplitude, ^a deg	Slope, K		Coulomb Friction, ^b CF		Angular velocity, ^a deg/sec
				J/deg	ft-lb/deg	J	ft-lb	
Ambient temperature and pressure								
759	Triangle	0.10	0.25	567	418	129	95	0.10
		.50	↓	544	401	118	87	.50
		1.00	↓	529	390	115	85	1.00
		2.00	↓	380	280	113	83	2.00
94	Triangle	0.10	2.00	939	693	125	92	0.80
		.50	↓	580	428	122	90	4.00
		1.00	↓	321	237	117	86	9.00
		2.00	↓	200	148	110	91	16.00
Ambient temperature and vacuum								
759	Triangle	0.10	2.00	603	445	87	54	0.30
		.50	↓	---	---	---	---	---
		1.00	2.00	194	143	75	55	9.00
		2.00	2.00	100	74	73	54	16.00
94	Triangle	0.10	2.00	1128	832	79	58	0.80
		.50	↓	389	287	85	53	4.00
		1.00	↓	274	202	88	65	9.00
		2.00	↓	160	118	85	63	16.00
Cryogenic temperature								
759	Triangle	0.10	0.25	1356	1000	122	90	0.10
		.50	↓	1017	750	115	85	.50
		1.00	↓	881	650	115	85	1.00
		2.00	↓	637	470	115	85	2.00
	Sine	0.10	0.25	1274	940	102	75	0.157
		.50	↓	915	675	↓	↓	.785
		1.00	↓	698	515	↓	↓	1.571
		2.00	↓	407	300	↓	↓	3.142
	Triangle	0.10	2.00	1152	850	34	25	0.80
		.50	↓	373	275	41	30	4.00
		1.00	↓	187	139	47	35	9.00
		2.00	↓	115	85	47	35	16.00
94	Triangle	0.10	0.25	1310	966	113	83	0.10
		.50	↓	1093	806	103	76	.50
		1.00	↓	626	462	98	72	1.00
		2.00	↓	504	372	98	72	2.00
	Sine	0.10	0.25	1474	1087	98	72	0.157
		.50	↓	1201	886	98	72	.785
		1.00	↓	1197	883	98	72	1.571
		2.00	↓	360	265	90	66	3.142
	Triangle	0.10	2.00	1316	971	58	43	0.30
		.50	↓	449	331	60	44	4.00
		1.00	↓	268	198	57	42	9.00
		2.00	↓	157	116	61	45	16.00

^aZero to peak.
^bPeak to peak.

TABLE II. - SUMMARY OF EXPERIMENTAL DATA IN YAW AXIS

Gimbal number	Waveform	Frequency, Hz	Amplitude, ^a deg	Slope, K		Coulomb friction, ^b CF		Angular velocity, ^c deg/sec
				J/deg	ft-lb/deg	J	ft-lb	
Ambient temperature and pressure								
759	Triangle	0.10	2.00	1108	817	201	148	0.80
		.50	↓	625	461	183	135	4.00
		1.00	↓	404	298	182	134	8.00
		2.00	↓	237	175	180	133	16.00
94	Triangle	0.10	2.00	834	615	113	83	0.80
		.50	↓	488	360	102	75	4.00
		1.00	↓	309	228	83	61	8.00
		2.00	↓	163	120	72	53	16.00
Ambient temperature and vacuum								
759	Triangle	0.10	2.00	1045	771	184	136	0.80
		.50	↓	675	498	174	128	4.00
		1.00	↓	361	266	172	127	8.00
		2.00	↓	225	166	168	124	16.00
94	Triangle	0.10	2.00	949	700	85	63	0.80
		.50	↓	442	326	79	58	4.00
		1.00	↓	259	191	75	55	8.00
		2.00	↓	144	106	68	50	16.00
Cryogenic temperature and vacuum								
759	Triangle	0.10	0.25	1017	750	203	150	0.10
		.50	↓	1003	740	201	148	.50
		1.00	↓	976	720	202	149	1.00
		2.00	↓	983	725	193	142	2.00
	Sine	0.10	0.25	1028	758	207	153	0.157
		.50	↓	891	657	205	151	.785
		1.00	↓	813	600	201	148	1.571
		2.00	↓	697	514	193	142	3.142
	Triangle	0.10	2.00	975	719	126	93	0.80
		.50	↓	487	359	102	75	4.00
		1.00	↓	324	239	99	73	8.00
		2.00	↓	168	124	98	72	16.00
94	Triangle	0.10	0.25	963	710	77	57	0.10
		.50	↓	831	613	68	50	.50
		1.00	↓	495	365	68	50	1.00
		2.00	↓	373	275	64	47	2.00
	Sine	0.10	0.25	893	659	69	51	0.157
		.50	↓	880	649	68	50	.785
		1.00	↓	675	498	65	48	1.571
		2.00	↓	363	268	61	45	3.142
	Triangle	0.10	2.00	1013	747	15	11	0.80
		.50	↓	335	247	14	10	4.00
		1.00	↓	187	138	14	10	8.00
		2.00	↓	95	70	12	9	16.00

^aZero to peak.
^bPeak to peak.

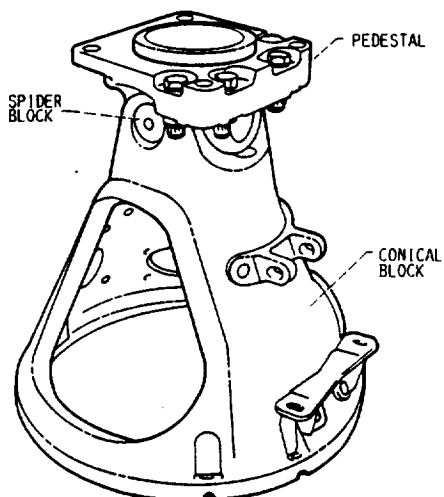


FIG. 1. - ENGINE MOUNT GIMBAL ASSEMBLY.

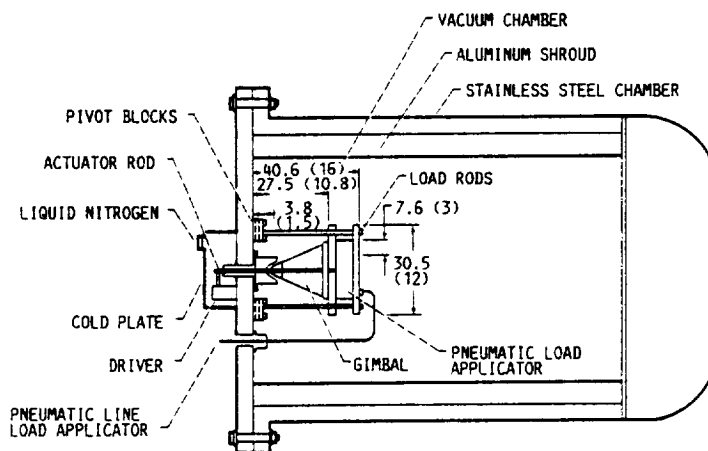


FIG. 2. - GIMBAL FRICTION TEST SETUP. (ALL DIMENSIONS GIVEN IN CM (IN.).)

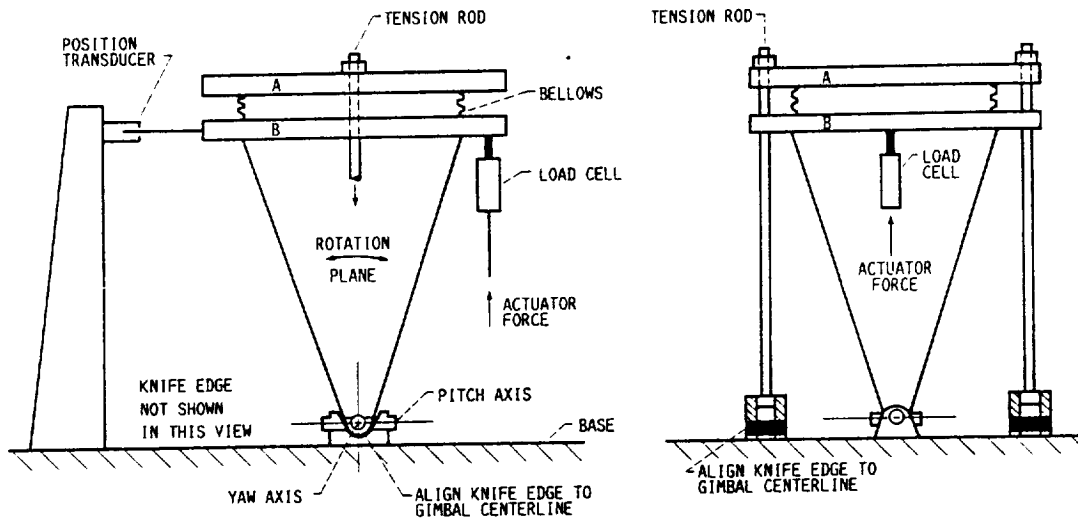


FIG. 3. - GIMBAL FRICTION TEST RIG CONFIGURATION.

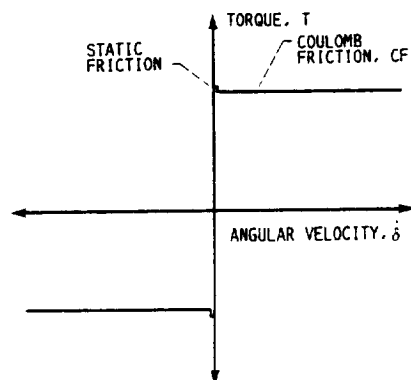


FIG. 4. - CONVENTIONAL DEFINITION OF SOLID FRICTION.

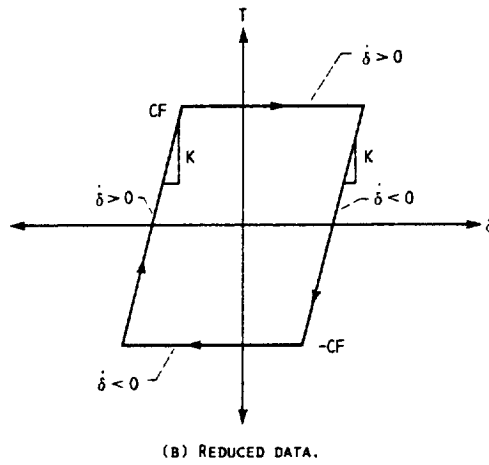
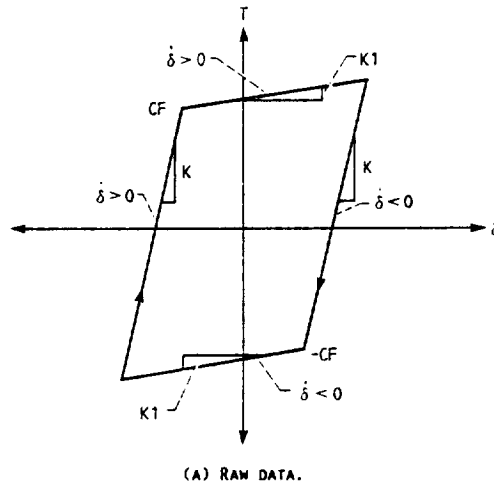
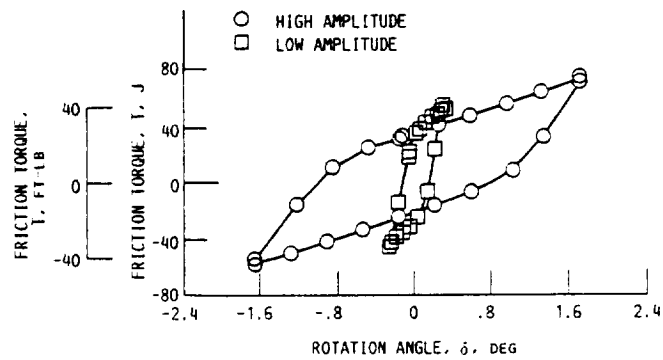


FIG. 5. - TORQUE AS A FUNCTION OF ROTATION
FOR RAW AND REDUCED DATA.



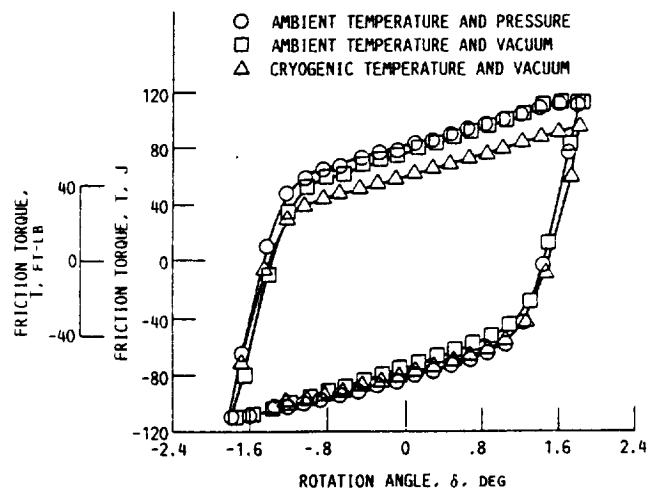


FIG. 7. - GRAPHICAL REPRESENTATION OF THE DIFFERENT TEST CONDITIONS AT $\pm 1.85^\circ$. FREQUENCY, 1.0 HZ; PITCH AXIS; TRIANGULAR WAVE INPUT.

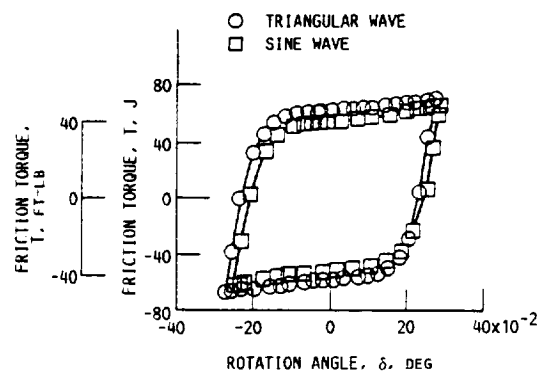


FIG. 8. - GRAPHICAL REPRESENTATION OF THE CHARACTERISTICS OF INPUT SIGNALS, AT 0.25° . FREQUENCY, 0.10 HZ; PITCH AXIS.

REPORT DISTRIBUTION LIST

NASA Lewis Research Center
21000 Brookpark Road
Cleveland, OH 44135

Attn: J. A. Burkhart/MS 500/120
T. P. Burke/MS 500-319
R. C. Oeftering/MS 500-107
S. R. Graham/MS 500-107 (3 copies)
A. J. Willoughby/Analox/MS 500-105
Library

NASA Headquarters
Washington, D.C. 20546

Attn: MSD/S. J. Cristofano
MSD/J. R. Lease
MS/J. B. Mahon
MTT/L. K. Edwards
RST/F. W. Stephenson
Library

General Dynamics Space Systems Division
P. O. Box 80847
San Diego, CA 92138

Attn: W. J. Ketchum
J. Rager
K. Allen
R. Beach
J. Cimenski
Library

Martin Marietta Corp.
P. O. Box 179
Denver, CO 80201

Attn: J. Bunting
Library

USAF Space Division
P. O. Box 92960
Worldway Postal Center
Los Angeles, CA 90009-2960

Attn: CLVD/Col. W. Anders
CL/Col. Hard
YXD/Maj. R. Proctor
YXD/Lt. J. Creamer
YXD/Capt. R. Soland
CLVD/Lt. Col. J. Rogers